AD-A126 322 MAGNETIZATION OF RARE EARTH/COBALT PERMANENT MAGNETS 1/1
SUBSEQUENT TO ASSEMB..(U) GENERAL ELECTRIC CO
BINGHAMTON N Y AEROSPACE CONTROLS AND ELE..
UNCLASSIFIED D N TANEJA ET AL. JUN 82 AES-14001 F/G 20/3 NL

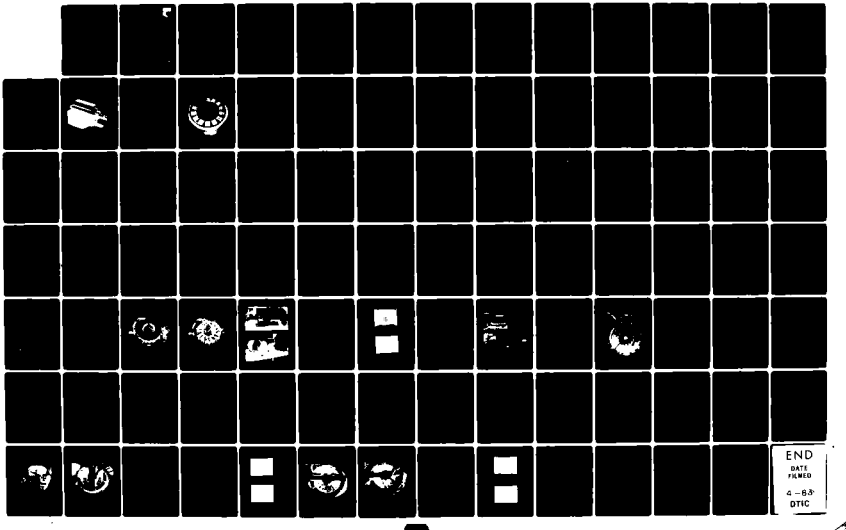

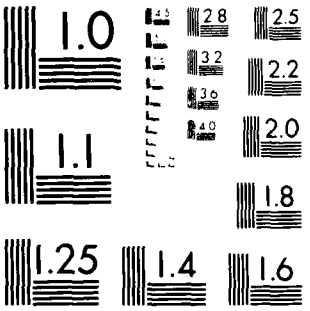

12

AFWAL-TR-82-2086

MAGNETIZATION OF RARE EARTH/COBALT PERMANENT MAGNETS SUBSEQUENT TO ASSEMBLY IN COMPLEX ROTOR STRUCTURES

D. N. TANEJA
R. C. WEBB
D. L. MARTIN

GENERAL ELECTRIC COMPANY
BOX 5000
BINGHAMTON, NEW YORK 13902

JUNE 1982

FINAL REPORT FOR PERIOD JULY 1979 – AUGUST 1981

APPROVED FOR PUBLIC RELEASE: DISTRIBUTION UNLIMITED

AERO PROPULSION LABORATORY
AIR FORCE WRIGHT AERONAUTICAL LABORATORIES
AIR FORCE SYSTEMS COMMAND
WRIGHT-PATTERSON AIR FORCE BASE, OHIO 45433

NOTICE

When Government drawings, specifications, or other data are used for any purpose other than in connection with a definitely related Government procurement operation, the United States Government thereby incurs no responsibility nor any obligation whatsoever; and the fact that the government may have formulated, furnished, or in any way supplied the said drawings, specifications, or other data, is not to be regarded by implication or otherwise as in any manner licensing the holder or any other person or corporation, or conveying any rights or permission to manufacture use, or sell any patented invention that may in any way be related thereto.

This report has been reviewed by the Office of Public Affairs (ASD/PA) and is releasable to the National Technical Information Service (NTIS). At NTIS, it will be available to the general public, including foreign nations.

This technical report has been reviewed and is approved for publication.

William V. Borger

WILLIAM U. BORGER
Acting Technical Area Manager
Power Systems Branch

David H. Schorr

DAVID H. SCHORR, Major, USAF
Chief, Power Systems Branch
Aerospace Power Division

FOR THE COMMANDER

D. David Randall

D. DAVID RANDALL, Major, USAF
Acting Chief, Aerospace Power Division
Aero Propulsion Laboratory

"If your address has changed, if you wish to be removed from our mailing list, or if the addressee is no longer employed by your organization please notify AFWAL/POOS, *W-PAFB, OH 45433 to help us maintain a current mailing list".*

Copies of this report should not be returned unless return is required by security considerations, contractual obligations, or notice on a specific document.

UNCLASSIFIED

SECURITY CLASSIFICATION OF THIS PAGE (When Data Entered)

REPORT DOCUMENTATION PAGE		READ INSTRUCTIONS BEFORE COMPLETING FORM
1. REPORT NUMBER AFWAL-TR-82-2086	2. GOVT ACCESSION NO. AD-A126 302	3. RECIPIENT'S CATALOG NUMBER
4. TITLE (and Subtitle) MAGNETIZATION OF RARE EARTH/COBALT PERMANENT MAGNETS SUBSEQUENT TO ASSEMBLY IN COMPLEX ROTOR STRUCTURES		5. TYPE OF REPORT & PERIOD COVERED FINAL July 79-August 81
		6. PERFORMING ORG. REPORT NUMBER AES 14001
7. AUTHOR(s) D.N. Taneja R.C. Webb D.L. Martin		8. CONTRACT OR GRANT NUMBER(s) F33615-79-C-2057
9. PERFORMING ORGANIZATION NAME AND ADDRESS General Electric Company P.O. Box 5000 Binghamton, N.Y. 13902		10. PROGRAM ELEMENT, PROJECT, TASK AREA & WORK UNIT NUMBERS P.E. 62203F, PROJ 31452960
11. CONTROLLING OFFICE NAME AND ADDRESS Aero Propulsion Laboratory (POO) Air Force Wright Aeronautical Lab (AFSC) Wright-Patterson AFB, OH 45433		12. REPORT DATE June 1982
		13. NUMBER OF PAGES 84
14. MONITORING AGENCY NAME & ADDRESS(if different from Controlling Office)		15. SECURITY CLASS. (of this report) Unclassified
		15a. DECLASSIFICATION/DOWNGRADING SCHEDULE

16. DISTRIBUTION STATEMENT (of this Report)

Approved for Public Release;
Distribution Unlimited

17. DISTRIBUTION STATEMENT (of the abstract entered in Block 20, if different from Report)

18. SUPPLEMENTARY NOTES

19. KEY WORDS (Continue on reverse side if necessary and identify by block number)

Magnetization - Permanent Magnets
Magnetoelectric Generators
Samarium
Cobalt - Transistion Metals

20. ABSTRACT (Continue on reverse side if necessary and identify by block number)

The object of this program was to demonstrate the feasibility of magnetizing large rare earth/cobalt permanent magnets subsequent to their assembly in complex rotor structures. A safe demagnetization (to near zero remanence) technique was optimized and demonstrated on individual magnets with insignificant detrimental affect on the magnet physical properties. Magnetic finite element analysis was completed which optimized the winding location requirements

DD FORM 1 JAN 73 1473 EDITION OF 1 NOV 65 IS OBSOLETE

UNCLASSIFIED

SECURITY CLASSIFICATION OF THIS PAGE (When Data Entered)

for the magnetization and substantiated that remagnetization of large rare earth/cobalt permanent magnets assembled in complex rotor structures is feasible if the magnetic field could be obtained. The demonstration of the remagnetization of large rare earth/cobalt permanent magnets assembled in complex rotor structures was not successful. This is a result of failure in the magnetization fixture structure. The failures were precipitated by the high magnetic field reactions and the confined space requirements.

PREFACE

This document is a technical report covering a two-phase program to demonstrate the feasibility of magnetizing large rare earth/cobalt permanment magnets subsequent to their assembly in complex rotor structures. This program is part of an overall Air Force effort to develop lightweight, low cost, high performance motors and generators for advanced aerospace applications. The work was performed by the Armament and Electrical Systems Department of the General Electric Company, Binghamton, New York under Air Force Contract No. F33615-78-C-2057.

The work was sponsored by the Aero Propulsion Laboratory, Air Force Wright Aeronautical Laboratories, Wright-Patterson Air Force Base, Ohio (45433) under Project 3145, Task 314529, Work Unit 31452960, with Dr. W.E. Borger, AFWAL/POOS-2 serving as Project Engineer.

The principal investigators were: Dr. Lou Martin from the General Electric Company, Corporate Research Center in Schnectady, New York who optimized the safe demagnetization technique; Dr. John Mallick from the General Electric Company, Corporate Research Center in Schnectady, New York who performed the magnetic finite element analysis; and Dinesh Taneja from the General Electric Company, Arament and Electrical Systems Department in Erie, Pennsylvania who designed, fabricated, and tested the complex rotor structure and magnetization fixture.

Also contributing to this effort as a consultant was Dr. Eike Richter from the General Electric Company, Corporate Research Center in Schnectady, New York and Victor Mishkousky of the General Electric Company's Wilfred F. Skeats Laboratory, Philadelphia, Pennsylvania.

Also contributing to the magnetization effort was LDJ Electronics in Troy, Michigan.

TABLE OF CONTENTS

Table of Contents (Continued)

LIST OF ILLUSTRATIONS

List of Illustrations (Continued)

List of Illustrations (Concluded

LIST OF TABLES

SECTION I

INTRODUCTION

1. INTRODUCTION

In the magnetized state, all permanent magnets have an attraction to other ferromagnetic materials. This attractive force causes magnetic debris to accumulate and stick to the surface of the magnet. Also, the magnetic attraction can cause the magnet to impact other magnetic parts if not properly handled causing the brittle magnet to fracture and become unusable. These problems are particularly serious with the relatively new rare earth/cobalt magnets which have an extremely high energy product (>15MGO$_e$) and are very brittle.

In the case of permanent magnet materials other than rare earth/cobalt, the above mentioned problems are sometimes avoided by handling the magnets in the demagnetized state. After assembly, the magnets are magnetized by the application of an external field of up to 20KO$_e$. This is a relatively low magnetizing field and can be attained easily in rather complex structures.

Rare earth/cobalt magnets have a very high coercive force (of the order of 15KO$_e$ to 30KO$_e$) in comparison to the other types of permanent magnets, see Figure 1. Magnet vendors, in order to assure total saturation during magnetization, use fields far in excess of 35KO$_e$. Attainment of this magnetization field is considered impractical when trying to achieve magnetization in a complex rotor structure; thus, the magnet has been purchased in the fully magnetized condition from the magnet vendor.

Rare earth/cobalt magnets as applied to the 150 KVA Variable Speed Constant Frequency (VSCF) Generator Rotor*, (see Figure 2) have demonstrated their capability and advantages in a high speed, high power density machine. The high energy product of these magnets (five times greater than other commercial magnets) is necessary to achieve the

*USAF Contract F33615-74-C-2037. See Final Program Report AFAPL-TR-78-104 for further details of design and construction.

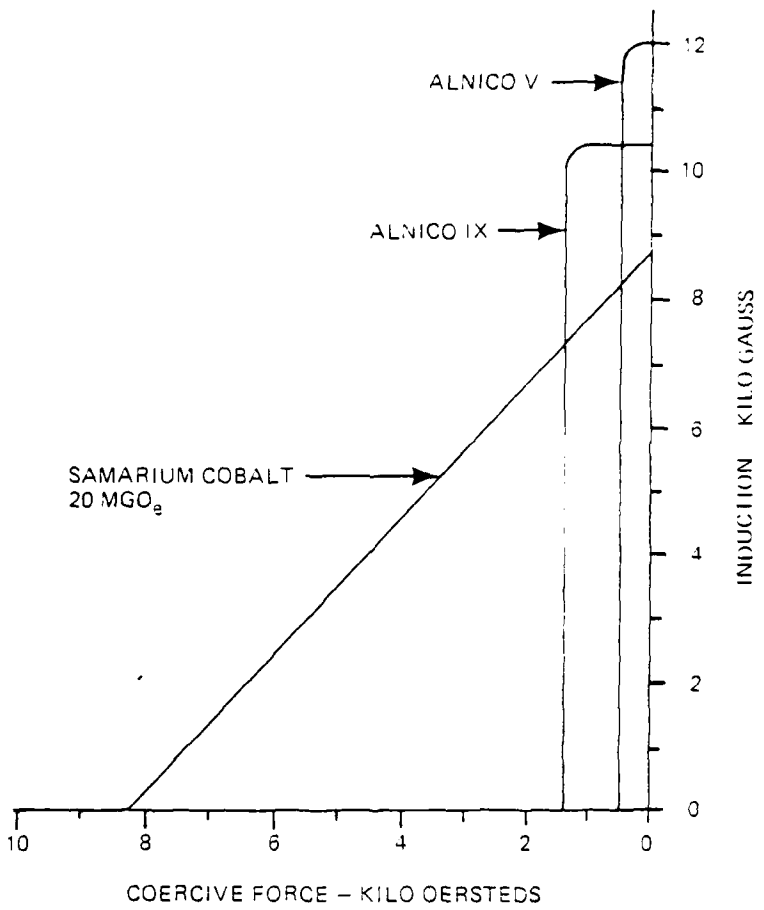

Figure 1. Magnet Comparison

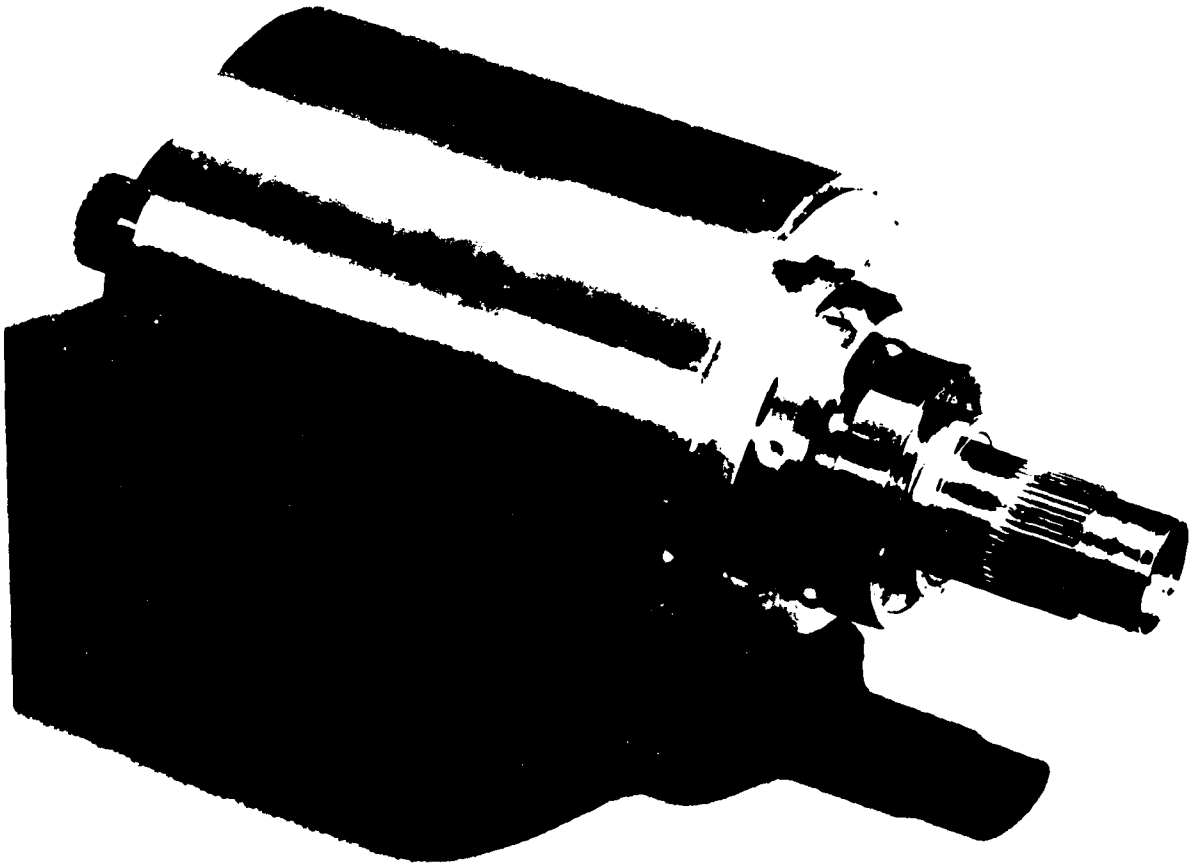

high power density machine. This high energy product is due to a very high intrinsic coercive force which is usually in excess of 15 K Oersteds (Oe).

Assembling a rotor, such as the 150 KVA VSCF rotor disc (see Figure 3) with fully magnetized magnets is difficult, time consuming and costly. The magnets attract or repel each other and are attracted to other magnetic parts of the rotor structure and the surrounding manufacturing area. When brought into close contact, the resulting forces can approach 40 pounds. This makes the magnets and magnet assemblies difficult to handle. If a magnet impacts other magnetic parts, the impact force can be large enough to cause the brittle magnet to break or chip making it unacceptable for use. Also, the magnets in the magnetized state attract small magnetic chips and particles, such as grinding dust, which are present in any rotating equipment manufacturing facility. These chips and particles are not easily removed and yet must be removed in each step of fabrication to meet strict assembly requirements.

Because of the above mentioned handling difficulties with rare earth/cobalt magnets in the magnetized state, it would be highly desirable to use magnets in the unmagnetized state during the fabrication of the rotor and to magnetize them in place after the assembly and machining is complete.

The objective of this program is: (1) to investigate and develop a process/procedure to demagnetize rare earth/cobalt magnets, (2) to minimize the loss of the capability after they have been characterized, and (3) minimize the field required to remagnetize these magnets. Then using these demagnetized magnets, demonstrate remagnetization after assembly in a complex rotor structure to achieve a maximum final magnetic property.

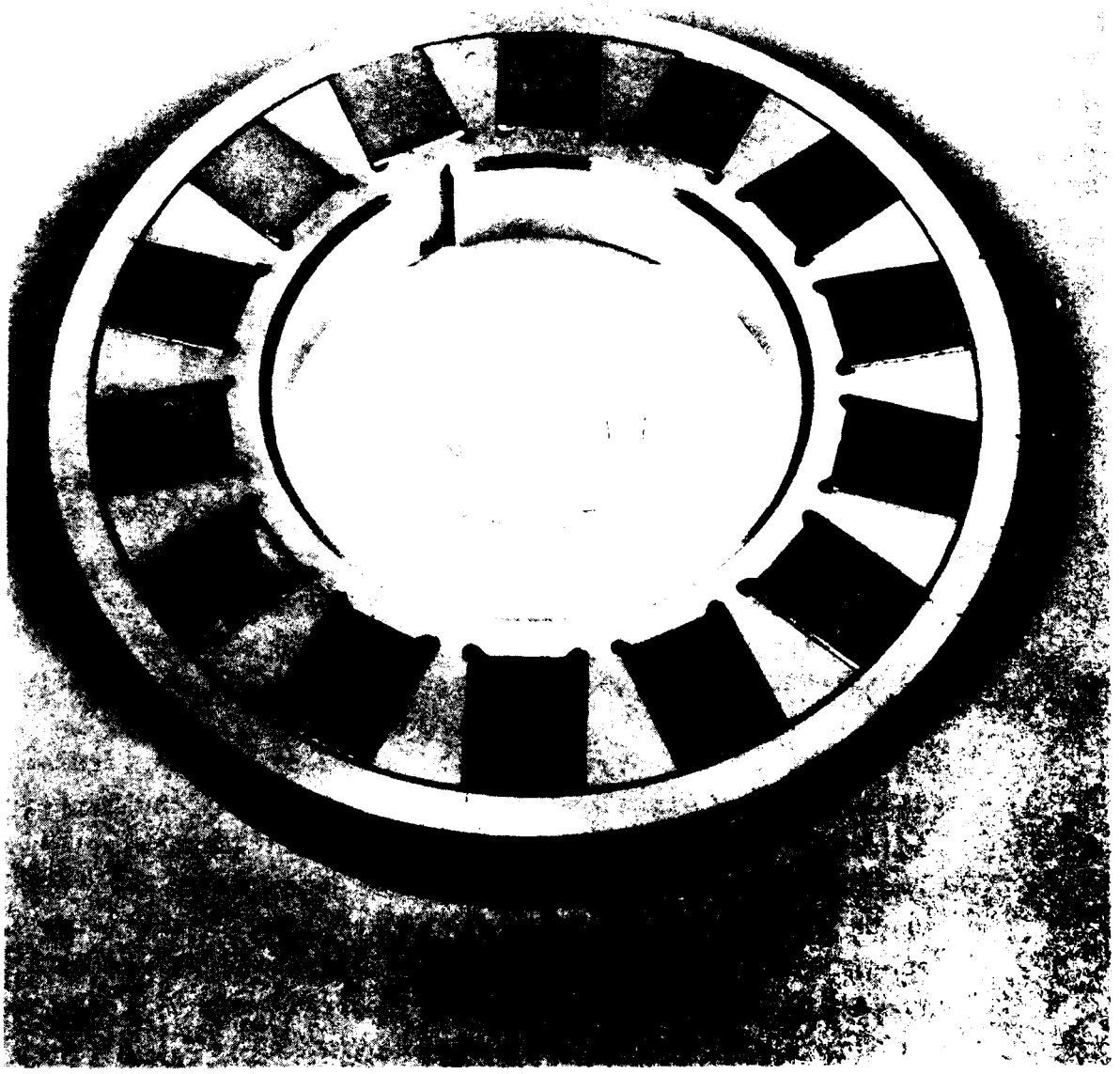

Figure 3. 150 KVA Rotor Disc

2. BACKGROUND

This report concludes a two-phase program to demonstrate the feasibility of magnetizing large rare earth/cobalt permanent magnets subsequent to their assembly in a complex rotor structure. Two separate technologies were pursued under this program. The first involved the optimization of a demagnetization technology to allow "safe" demagnetization (to near zero remanence) of previously magnetized rare earth/cobalt magnets. A "safe" demagnetization procedure is considered to be one that allows for remagnetization of the magnets to near full strength with field levels not exceeding those required for virgin magnets. This "safe" demagnetization procedure must also not detrimentally effect the physical properties of the magnets. The second technology area pursued was the design and fabrication of a fixture to remagnetize the magnets subsequent to their assembly in a rotor structure.

The first phase was comprised of two tasks. The following is a list of items under these tasks:

TASK 1 - "SAFE" DEMAGNETIZATION PROCEDURE

- o Define and optimize the temperature and field conditions required to homogeneously reduce the magnetization to less than 500 gauss.
- o Measure and minimize the non-recoverable, irreversible losses due to oxidation and other structural changes.
- o Measure and optimize the second quadrant (B vs H) properties as a function of the remagnetizing field.
- o Study the effect of the thermal demagnetization treatment on the compressive load carrying capacity of the magnets, in particular to show that no significant change results from the thermal demagnetization treatment.
- o Based on the above results, generate a preliminary magnet specification for demagnetization and remagnetization treatment and the properties of a virgin magnet to be used in future magnetization in place effort.

- o Apply this process specification on 16 magnets for assembly and test in a single rotor disc from the 150 KVA Program.

TASK 2 - FIXTURE DESIGN

- o Design a fixture to remagnetize the 150 KVA rotor disc assembly
- o Design a fixture to measure the magnetized 150 KVA rotor disc assembly

The second phase was comprised of three tasks. They were:

Task 1 - Fabricate fixtures
- o Magnetization
- o Test

Task 2 - Remagnetization
- o Assemble rotor disc with demagnetized magnets
- o Magnetize disc with magnetization fixture

Task 4 - Test
- o Measure rotor disc magnetized after assembly
- o Measure rotor disc assembled with magnetized magnets

3. PROBLEM SOLUTION DISCUSSION

Generally, one of two procedures is used to demagnetize permanent magnets. A brief discussion follows on these methods and why they can not be applied to rare earth/cobalt magnets.

The most common method to demagnetize magnets is to expose the magnet to an alternating field whose initial peak value is somewhat greater than the intrinsic coercive force (H_{ci}) of the magnet (i.e., 0.5 KO_e to 5KO_e) and whose amplitude decreases to zero with time. In practice, this is done simply by passing the magnet through an ac solenoid. This approach does not work well with rare earth/cobalt magnets because of the high coercive force required. Either a large electromagnet or a superconducting magnet would have to be used to generate this field. The large field required combined with the rate at which

these field sources must be reversed makes this approach impractical. This approach has been tried on rare earth/cobalt magnets but the magnets did not become fully demagnetized. Large macroscopic regions remained that were still magnetized. The problems of magnetic dirt and impact fractures were reduced but not removed completely. Thus, this method does not meet program objectives.

The second method common for demagnetizing a magnet is to expose it to a temperature above its Curie temperature. If the magnet is not exposed to a magnetic field while cooling, the magnet will be in a fully demagnetized state, both macroscopically and microscopically. This is true of rare earth/cobalt magnets as well as other magnets.

Thus, thermal demagnetization above the Curie temperature appears to be a satisfactory approach to fully demagnetize rare earth/cobalt magnets. However, heating above the Curie temperature changes the final coercive force requiring extremely high magnetizing forces to realign the magnetic domains in rare earth/cobalt magnets. The coercive force and the demagnetization characteristics are strongly dependent upon the rate of cooling from 875°C to 500°C. If the magnet is demagnetized by this method, the resulting magnetic properties may vary widely. In some applications this variation in magnetic properties could be tolerated. In the complex rotor considered, magnets of high energy product are desirable. Therefore, until sufficient manufacturing experience and testing has demonstrated closely reproducible properties on quenching from above 875°C, this approach to demagnetization is unacceptable.

A third demagnetization approach has been identified for rare earth/cobalt magnets which appears to satisfy the requirements of low field for remagnetization (around $20KO_e$) and predictable properties. In this approach, the rare earth/cobalt magnetized magnet is subjected to a moderate, elevated temperature (400-500°C) and a moderate demagnetizing field, about 1000 Oe. The cooling rate from this exposure is unimportant. The remagnetized magnet properties are virtually

identical to the initial properties. This method for demagnetizing rare earth/cobalt magnets was patented (U.S. Patent 3,802,935 assigned to the General Electric Company) by Martin and Parker in April 1974.

Microscopic examination of the demagnetized magnet by this process reveals that the magnetic domain structure is nearly identical to a magnet that has been exposed to temperatures above its Curie temperature, thus giving total demagnetization. The important feature different from Curie temperature demagnetization lies in the domain structure. Each grain contains several domains and the domain walls are not pinned by the grain boundaries. Therefore, the initial coercive force and field required for magnetization is low. The 500°C exposure does not appear to affect the microstructure which controls the remagnetization coercive force.

4. TECHNICAL APPROACH PURSUED

The third approach described above was selected as the prime candidate to meet the objective contained in Section F of the contract. This approach provided the essential method to "demonstrate the feasibility of magnetizing large rare earth/cobalt magnets subsequent to their assembly in complex rotor structures."

SECTION II

SUMMARY

1. OVERVIEW

The overall program addressed the magnetization of rare earth/cobalt permanent magnets subsequent to their assembly in complex rotor structures. The particular complex rotor structure used for this program was a 14-pole disc that used circumferentially oriented magnets of <20 million gauss oersted energy product. This arrangement is shown in Figure 4. This rotor assembly had the following features:

- o An air gap density equal to a wire wound excited machine
- o Excellent resistance to demagnetization from armature reaction
- o Containment structure designed for high tip velocities. <750 Feet/second
- o Highest quality and highest energy product magnets available at the time of procurement (Magnets from this time period were around a nominal value of 17 million gauss oersteds.)

The above listed features are the characteristics for a particular rotor structure that provides an extremely rugged design. This particular rotor design was selected because it was considered to be the most difficult to remagnetize. Alternate rotor configurations could be realized that would enable magnetization after assembly to be accomplished more readily but would compromise the selected design's rugged features.

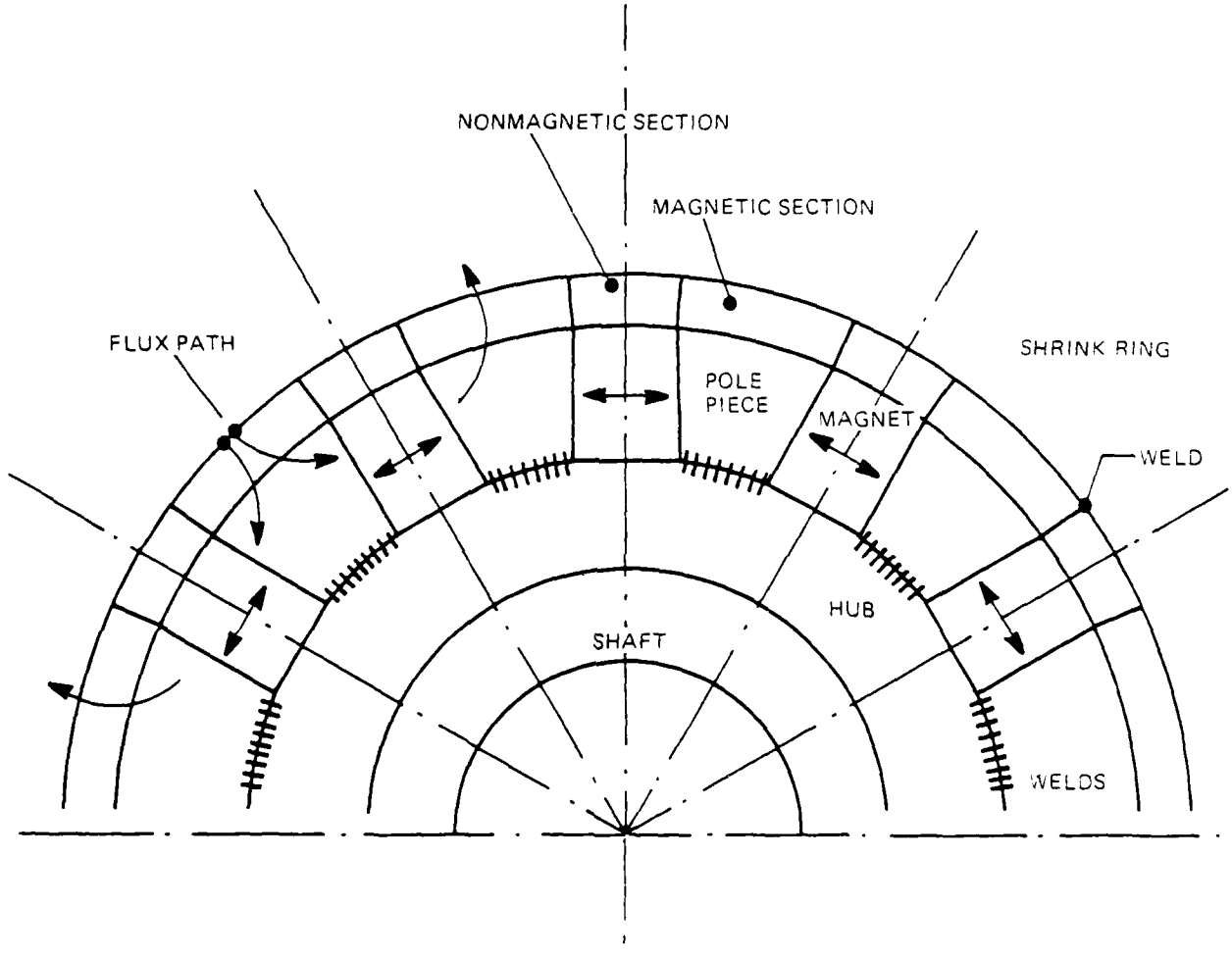

Figure 4. Rotor Disc Magnetic Cross Section

2. PHASE I SUMMARY - DEMAGNETIZATION DEVELOPMENT/FIXTURE DESIGN

The feasibility of a process for thermal demagnetization and then remagnetizing to an acceptable level of magnetic quality was demonstrated. The demagnetization process consisted of heating to a temperature near 450°C in the presence of a 1250 oersted demagnetizing field before cooling to room temperature. The residual magnet magnetization after treatment was ±5% of its starting value. A remagnetization field goal of 25-30 Kilo oersteds was selected as providing maximum recovery at a level attainable in the remagnetization fixture.

Forty magnets were measured for their B:H characteristics. It was shown that either the magnetic open circuit induction value or the open circuit magnetization value could be used for the (BH) max evaluation purposes.

The test of compressive strength of the thermally demagnetized magnets showed no degradation of the magnet's physical properties. Thus, the thermal demagnetization process did not affect the physical properties of the magnets.

Normal magnetization calculations were completed which indicated magnetization of the complex rotor structure was feasible with a commercially available power supply. Detail drawings of the magnetizing and measuring fixtures were completed.

3. PHASE II SUMMARY - FIXTURE FABRICATION/REMAGNETIZATION/TEST

Difficulties in attaining the desired levels of magnetization were encountered. Detailed magnetic Finite Element Analysis (FEA) techniques were employed which enabled the magnetization fixture winding location and magnetization current requirements to be optimized. The FEA analysis conducted predicted magnetization of a complex rotor structure was feasible if the magnetization current level could be attained.

The magnetization fixture was redesigned and a larger pulse type power supply was used.

Ultimate demonstration of the magnetization of a complex rotor structure was not demonstrated. The combination of high current (forces) in a confined area prohibited the magnetization fixture windings from withstanding the current pulses. Further magnetization effort was not completed due to the fixture failure and depletion of program funds.

SECTION III

PROGRAM RESULTS

1. INTRODUCTION

The following details the work accomplished on this program. This effort has been divided into Phase I and Phase II details to enable the required effort to be better identified in this report.

2. PHASE I - DEMAGNETIZATION DEVELOPMENT AND FIXTURE DESIGN

a. Demagnetization Development

The objective of this part of the program was to demonstrate the feasibility of demagnetizing the cobalt-samarium magnets after testing and to demonstrate that the demagnetized magnets can be remagnetized to meet the specifications.

The following tasks are covered in this section:

- Measurement of the B:H characteristics of the 40 magnets from AF Contract F33615-74-C-2037
- Measure the magnetization level of the magnets at 205 $\pm 5^{o}C$.
- Determine a safe demagnetization procedure that does not degrade magnetic properties.
- Determine the magnetic characteristics of the magnets after demagnetization. Demagnetize at field levels "near" the expected fixture field levels in order to determine the sensitivity of remanence to applied field.

- Measure the room ambient, 29 $\pm 5^{o}$C, compression strength of the demagnetized magnets in a direction perpendicular and parallel to the alignment direction to determine whether the mechanical properties have been degraded by the demagnetizing process.

- Demagnetize the 16 magnets to be used in Phase II of the program.

(1) Magnetic Characterization of the As-Received Magnets

The magnets used have nominal dimensions of 1 inch by 0.930 inch by 0.760 inch. The direction of magnetic alignment is parallel to the 0.760 inch direction. The average volume is 0.705 cubic inch or 11.56 cm^3. Because of the magnet size, it was not possible to use the normal test method involving extraction of the specimen from a pickup coil located in a superconducting solenoid.[1] Instead, a combination of methods were used. The open-circuit magnetization, $4\pi J_o$, was measured by pulling the magnet out of the center of Helmholtz coils,[2,3] and the B_o and B_r induction values were determined by use of a close-fitting pickup coil.

The magnetization was calculated from the following:

$$4\pi J_o = \frac{C \times \text{Fluxmeter Deflection}}{\text{Volume}}, \text{ gauss} \qquad (1)$$

where C is a calibration constant for the Helmholtz coils and the fluxmeter. The Helmholtz coils were about 12 inches in diameter.

The B_r and B_o values were obtained by using an electromagnet, a close-fitting search coil and an integrating voltmeter. The procedure followed was to place the premagnetized magnet and surrounding coil in an

electromagnet, increase the field to a positive value of about 15 KOe, then decrease the field to a zero value. The $\int edt(1)$ value is measured when the coil and magnet are pulled out of the electromagnet at the same time that the pole faces are opened slightly. Next the coil is pulled off the sample and the open circuit $\int edt(2)$ value is measured. The B_o and B_r values are determined from these two integrated voltage values (millivolt-seconds) as follows:

$$B_o = \frac{10^5 (\int edt(2))}{n A_s}, \text{ gauss} \qquad (2)$$

and

$$B_r = \frac{10^5 (\int edt(1) + \int edt(2))}{n A_s}, \text{ gauss} \qquad (3)$$

where n is the number of turns in the search coil and A_s is the cross-sectional area of the sample in cm^2.

Figure 5 gives a typical plot of the data for one of these magnets. These test methods work very well for rare earth/cobalt permanent magnets because of the linear relationship between B_r and H_c. The load line or permeance line slopes were determined from the dimensions of the magnet and by use of Joseph's demagnetization factors.[4] For determinating the length to diameter ratio, the assumption was made that the effective diameter was that of a circle equal in area to that of the 1 inch by 0.930 inch rectangle.

The point J_2 in Figure 5 was obtained by measuring the open-circuit magnetization with the Helmholtz coil system and by use of equation 1 above. The point J_3 was obtained in a similar manner after exposing the magnet to a known demagnetizing field, H_3. The line $J_3 - H_3$ is parallel to the line $J_2 - H_o$.

The second quadrant B:H data for 38 magnets measured are given in Table 1 (two magnets were broken during testing, illustrating the problem of handling magnetized magnets). Histograms for B_r, H_c and

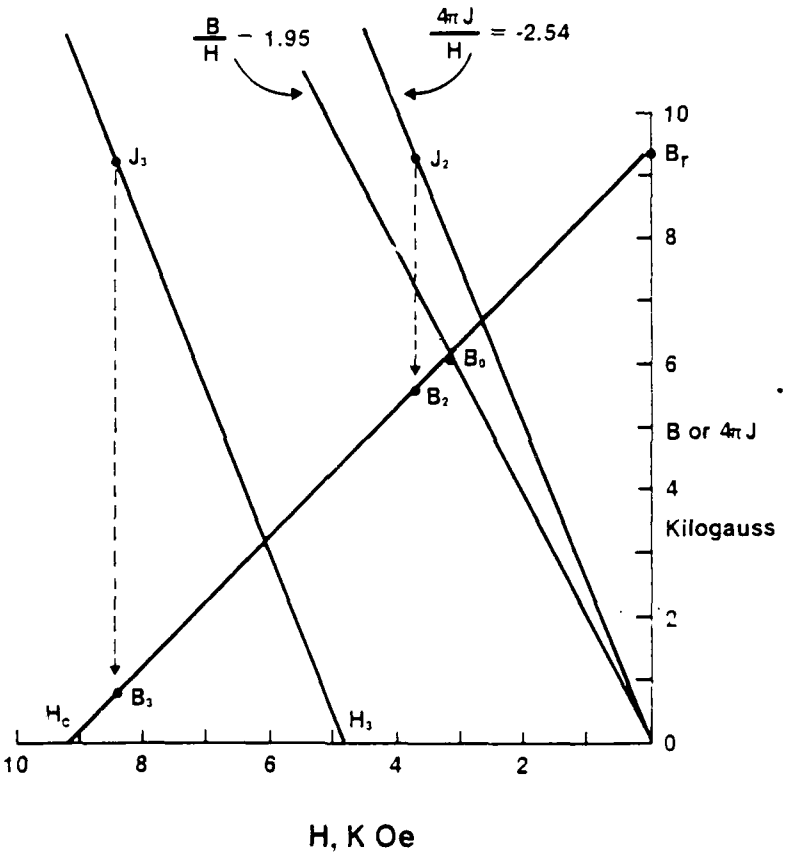

Figure 5. B:H Curve Construction Detail

TABLE 1

B:H PROPERTIES OF THE AS-RECEIVED MAGNETS

No.	B_r Kilogauss	H_c KOe	$(BH)_{max}$ MGOe	B_o Kilogauss	$4\pi J_o$ Kilogauss
12	9.4	9.2	21.5	6.1	9.2
14	9.5	8.9	21.0	6.0	9.3
18	9.5	9.0	21.4	6.1	9.4
33	9.4	8.6	20.3	6.0	9.2
87	9.3	8.7	20.4	5.9	9.1
112	9.2	8.9	20.5	5.8	9.1
153	9.5	9.0	21.3	6.0	9.4
156	9.3	9.0	20.7	5.9	9.2
157	9.3	9.1	21.2	6.0	9.3
158	9.5	8.8	20.7	6.0	9.3
159	9.1	8.9	20.3	5.9	9.1
181	9.3	9.0	21.0	5.9	9.3
182	9.3	8.9	20.5	5.9	9.2
189	9.4	9.1	21.3	6.0	9.3
201	9.3	9.1	21.2	6.0	9.3
283	9.3	9.2	21.2	6.0	9.2
292	9.0	9.0	20.3	5.9	9.0
294	9.0	9.0	20.4	5.9	9.0
301	9.4	9.0	21.1	6.0	9.2
303	9.4	9.1	21.3	6.1	9.3
310	9.3	9.1	21.3	6.1	9.3
315	9.0	8.8	19.7	5.9	9.0
321	9.5	9.1	21.7	6.1	9.3
330	9.5	9.3	22.1	6.2	9.5
333	9.6	9.2	22.0	6.1	9.4
340	9.5	9.3	22.0	6.1	9.5
343	9.5	9.2	21.7	6.1	9.4
345	9.3	9.0	20.9	6.0	9.2
346	9.4	9.1	21.3	6.0	9.3
348	8.9	8.6	19.1	5.8	8.8
351	9.4	9.1	21.4	6.1	9.3
354	9.1	8.9	20.3	5.9	9.0
358	9.7	9.3	22.6	6.3	9.6
367	9.4	9.1	21.3	6.1	9.3
371	9.7	9.4	22.8	6.3	9.6
380	9.6	9.4	22.5	6.2	9.5
382	9.5	9.3	22.1	6.2	9.4
387	9.5	9.3	22.2	6.2	9.4
Mean	9.4	9.0	21.2	6.0	9.3

$(BH)_{max}$ are given in Figure 6. Six of the magnets failed to meet the B_r specification of 9200 gauss and two magnets failed to meet the 20 MGOe specification for $(BH)_{max}$. Sixteen magnets were selected from the 38 magnets for the Phase II studies. The properties of Group A magnets are listed in Table 2, and compared to the 38 Group B magnets in Table 3. The mean values of the Group A magnets were upgraded by selection.

(2) 205°C Magnet Measurements

The measurements of the magnetic properties at 205°C were made in a small furnace, located inside the Helmholtz detection coils. The temperature was controlled to ± 2°C in the range 200° to 204°C. The procedure followed was to first measure the open-circuit magnetization at room temperature in another set of Helmholtz coils, heat the specimen to about 205°C, measure the magnetization after holding for several hours, cool the specimen to room temperature, and remeasure $4\pi J_o$. From these measurements the irreversible loss and the temperature coefficient of magnetization were determined. A summary of the data for the 38 magnets is given in Table 4 and for the selected Group A magnets in Table 5. Comparison of the mean values for the two groups is made in Table 6. The Group A magnets have slightly higher $4\pi J_o$ values at 205°C, lower irreversible losses and about the same reversible temperature coefficient.

(3) Demagnetization Studies

As discussed in Paragraph 3 of Section I, a magnetized permanent magnet can be demagnetized by thermal methods, by applying a demagnetizing field or by combinations of field and temperature. In the following sections discussions and results for these methods are given.

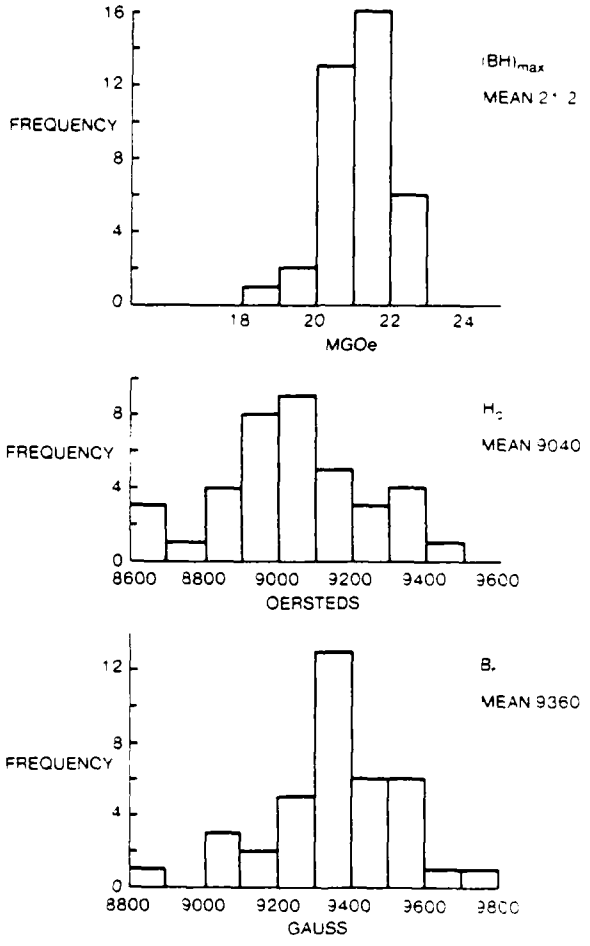

Figure 6. Histograms of Magnets Used

TABLE 2

B:H PROPERTIES OF GROUP A MAGNETS

No.	B_r Kilogauss	H_c KOe	BH_{max} MGOe	B_o Kilogauss	$4\pi J_o$ Kilogauss
18	9.4	9.2	20.9	6.1	9.4
157	9.3	9.1	21.2	6.0	9.3
189	9.4	9.1	21.3	6.0	9.3
201	9.3	9.1	21.2	6.0	9.3
283	9.3	9.2	21.2	6.0	9.2
303	9.4	9.1	21.3	6.1	9.3
310	9.3	9.1	21.3	6.1	9.3
321	9.5	9.1	21.7	6.1	9.3
333	9.6	9.2	22.0	6.1	9.4
340	9.5	9.3	22.0	6.1	9.5
346	9.4	9.1	21.3	6.0	9.3
351	9.4	9.1	21.4	6.1	9.3
358	9.7	9.3	22.6	6.3	9.6
367	9.4	9.1	21.3	6.1	9.3
382	9.5	9.3	22.1	6.2	9.4
387	9.5	9.3	22.2	6.2	9.4
Mean	9.4	9.2	21.6	6.1	9.4

TABLE 3

COMPARISON OF GROUP A MAGNETS WITH GROUP B MAGNETS

	Group A	Group B
No. of Magnets	16	38
Mean B_r	9.4	9.4
Mean H_c	9.2	9.0
Mean BH_{max}	21.6	21.2
Mean B_o	6.1	6.0
Mean $4\pi J_o$	9.4	9.3

TABLE 4

MAGNETS - 205°C MEASUREMENTS

Group No.	$4\pi J_o$ As Rec'd	$4\pi J_o$ After 30K0e	$4\pi J_o$ At °C		$4\pi J_o$ At RT After 205°C	% Irreversible Loss	Reversible Temp. Coeff.%
12	9180	9185	8055	200	8857	3.5	0.051
14	9295	9310	8230	204	9075	2.4	0.051
A 18	9405	9346	8332	202	9185	2.3	0.052
33	9185	8981	7920	204	8748	2.6	0.052
87	9115	9112	8105	204	8894	2.4	0.049
112	9115	9098	8126	203	8959	1.7	0.052
153	9405	9368	8342	203	9199	2.2	0.052
156	9150	8908	8023	203	8857	3.2	0.052
A 157	9260	9200	8300	203	9113	1.6	0.050
158	9260	9200	8300	203	9127	1.4	0.050
159	9060	8894	7940	204	8820	2.6	0.055
181	9285	9134	8177	203	9054	2.5	0.054
182	9185	-	-	-	-	-	-
A 189	9260	9260	8260	203	9047	2.3	0.048
A 201	9295	9273	8375	203	9185	1.2	0.049
283	9220	9185	8270	203	9112	1.2	0.051
292	9005	8748	7869	203	8660	3.8	0.051
294	9040	8855	7920	203	8784	2.8	0.055
301	9185	-	-	-	-	-	-
A 303	9300	9290	8330	204	9113	2.0	0.048
A 310	9300	9280	8280	202	9185	1.2	0.055
315	8970	8963	8025	202	8755	2.4	0.047
A 321	9345	9302	8404	202	9222	1.3	0.050
330	9475	-	-	-	-	-	-
A 333	9405	9405	8177	202	9005	4.3	0.051
A 340	9460	9427	8455	204	9330	1.4	0.052
343	9405	9435	8485	204	9295	1.2	0.048
345	9185	9170	8179	202	9040	1.6	0.053
A 346	9330	9310	8352	203	9192	1.5	0.051
348	8785	8384	7509	203	8310	5.4	0.054
A 351	9330	9330	8383	203	9220	1.2	0.051
354	9040	9040	8147	200	8960	0.9	0.051
A 358	9610	9623	8620	204	9426	1.9	0.047
A 367	9260	9295	8332	204	9149	1.2	0.049
371	9585	9404	8177	203	9010	6.0	0.051
380	9475	9470	8496	202	9368	1.1	0.052
A 382	9440	9411	8414	204	9222	2.3	0.048
A 387	9440	9404	8435	204	9258	1.9	0.049
Mean	9264	9200	8220		9055	2.2	0.051

Note: Sixteen magnets were selected from the 40 magnets initially characterized. Sixteen magnets were selected for Group A with the remainder of magnets becoming Group B.

TABLE 5

GROUP A MAGNETS - 205°C MEASUREMENT

Group No.	$4\pi J_o$ As Rec'd	$4\pi J_o$ After 30K0e	$4\pi J_o$ At °C		$4\pi J_o$ At RT After 205°C	% Irreversible Loss	Reversible Temp. Coeff. %
18	9405	9346	8332	202	9185	2.3	0.052
157	9260	9200	8300	203	9113	1.6	0.050
189	9260	9260	8260	203	9047	2.3	0.048
201	9295	9273	8375	203	9185	1.2	0.049
283	9220	9185	8270	203	9112	1.2	0.051
303	9300	9290	8330	204	9113	2.0	0.048
310	9300	9280	8280	202	9185	1.2	0.055
321	9345	9302	8404	202	9222	1.3	0.050
333	9405	9404	8177	202	9005	4.3	0.051
340	9460	9427	8455	204	9330	1.4	0.052
346	9330	9310	8352	203	9192	1.5	0.051
351	9330	9330	8383	203	9220	1.2	0.050
358	9610	9623	8620	204	9426	1.9	0.047
367	9260	9295	8332	204	9149	1.2	0.049
	9440	9411	8414	204	9222	2.3	0.048
387	9440	9404	8435	204	9258	1.9	0.049
Mean	9354	9334	8356		9182	1.9	0.050

TABLE 6

COMPARISON OF GROUP A AND GROUP B MAGNETS - 205°C

Mean $4\pi J_o$	As Received	At 205°C	After Exposure at 205°C
Group A	9354	8356	9182
Group B	9264	8220	9055

Irreversible Loss (25°C to 205°C)	
Group A	1.8%
Group B	2.2%

Reversible Temperature Coefficient, α (25°C to 205°C)	
Group A	0.050% Per °C
Group B	0.051% Per °C

THERMAL DEMAGNETIZATION ABOVE THE CURIE TEMPERATURE

A ferromagnetic material becomes paramagnetic when heated above its Curie temperature. Thus, heating a magnet above its Curie temperature is a very effective way to demagnetize a magnet. Upon cooling back to room temperature multidomains form within the grains as shown in Figure 7A for a rare earth/cobalt permanent magnet heated to 900°C. Note that the multidomain structure is very uniform throughout the area of the micrograph, thus yiedling a net magnetization of zero or nearly zero. Figure 7B gives the domain structure of a magnetized magnet. The domain structure is quite different, with very few multidomain grains.

One problem with thermal demagnetization of rare earth/cobalt magnets above the Curie temperature (above 750°C) is that there is a danger of degrading the properties of some of the magnets due to the critical nature of the treatment in regards to temperature, time, heating rate, and cooling rate. Consider, for example, the histogram in Figure 8 for the $4\pi J_o$ values of 109 magnets (these magnets were the original population from which the 40 used in this study were obtained). Six of the 109 magnets failed to meet the B_r specifications of 9200 gauss ($4\pi J_o$ values are actually slightly lower than B_r, Table 1, so this statement is not necessarily correct; however, it illustrates the point). If the six magnets were rejected and the remaining 103 magnets retreated by heating above the Curie temperature, it is expected that a distribution of $4\pi J_o$ similar to that in Figure 8 would be obtained and that another 6% of the magnets would fall below the specification value. Therefore, this thermal demagnetization treatment is not considered a safe demagnetization treatment for these magnets. However, if the specification value was 8700 gauss, then a thermal treatment above the Curie temperature could be used with a higher degree of confidence that the demagnetized magnets would meet the specification.

A

B

900° DEMAGNETIZATION

MAGNETIZED MAGNET

Figure 7. Magnet Domain Structure

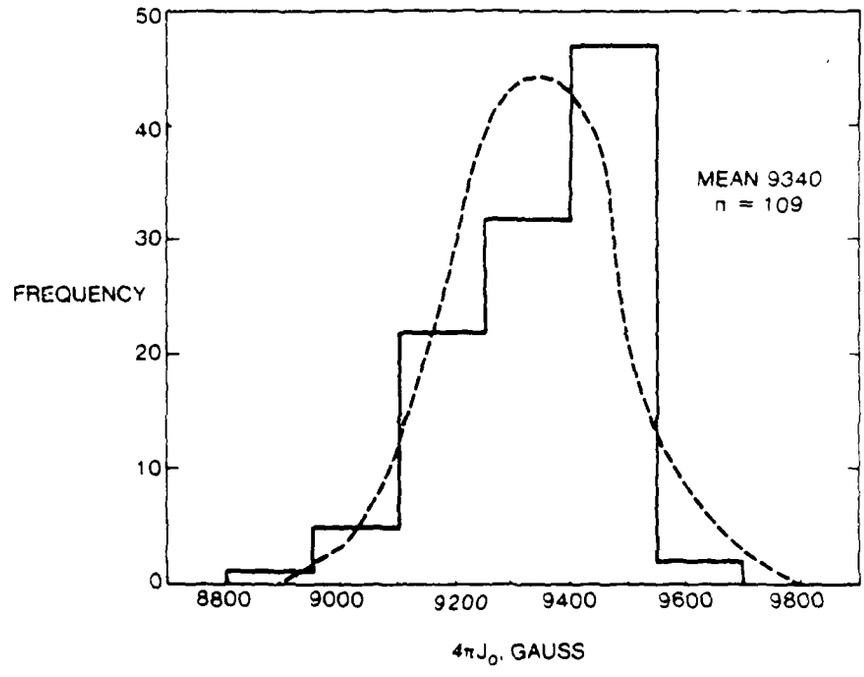

Figure 8. Histogram of Open Circuit Magnet Measurements

MAGNETIC FIELD DEMAGNETIZATION

Demagnetization by a magnetic field requires a field greater than the intrinsic coercive force. The method is illustrated in Figure 9. A field greater than 10,000 Oersteds is needed to drive the induction to point D. Upon removal of the field, the induction recoils to zero as shown. However, it can be seen that the value of field to achieve zero induction is critical, and a slightly lower or higher field would result in a partially magnetized magnet. This method requires a trial and error approach, and since there is a wide distribution of coercive force (Figure 6) for a batch of magnets, each magnet would require its own critical field for demagnetization. In addition, this method does not result in the formation of a uniform multidomain structure, but in domain reversals of macroscopic regions. Therefore, the method does not appear attractive for demagnetizing large numbers of those magnets being considered. For magnets with a much lower coercive force, such as Alnico 5, an ac field of decreasing amplitude is a satisfactory method of demagnetization.

THERMAL DEMAGNETIZATION BELOW THE CURIE TEMPERATURE

The basis for a process of thermal demagnetization below the Curie temperature is the observation that the intrinsic coercive force of rare earth/cobalt magnets decreases with increasing temperature and approaches zero above 400°C.[5,6] This is shown in Figure 10. Thus, heating a magnetized Co-Sm magnet above 400°C should result in some degree of demagnetization due to self-demagnetization associated with a decrease of coercive force. Such demagnetization does occur, as is shown in Figure 11 for magnets heated in the range of 450 to 550°C. Without a field, a temperature of 550°C is needed to decrease the $4\pi J_o$ value below 5% of the initial value at 25°C. A combination of temperature and a demagnetizing field of 1000 Oersteds shifts the curve to lower temperatures as shown in Figure 11. This is an important shift since metallurgical changes occur in the 500°C range which

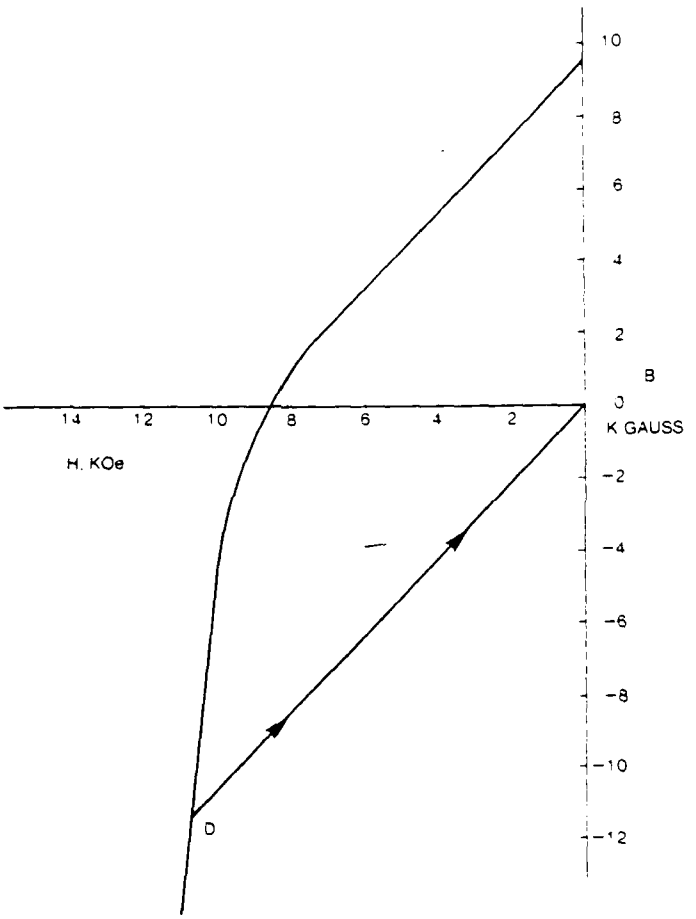

Figure 9. Second and Third Quadrants B:H Curve for a Rare Earth/Cobalt Magnet

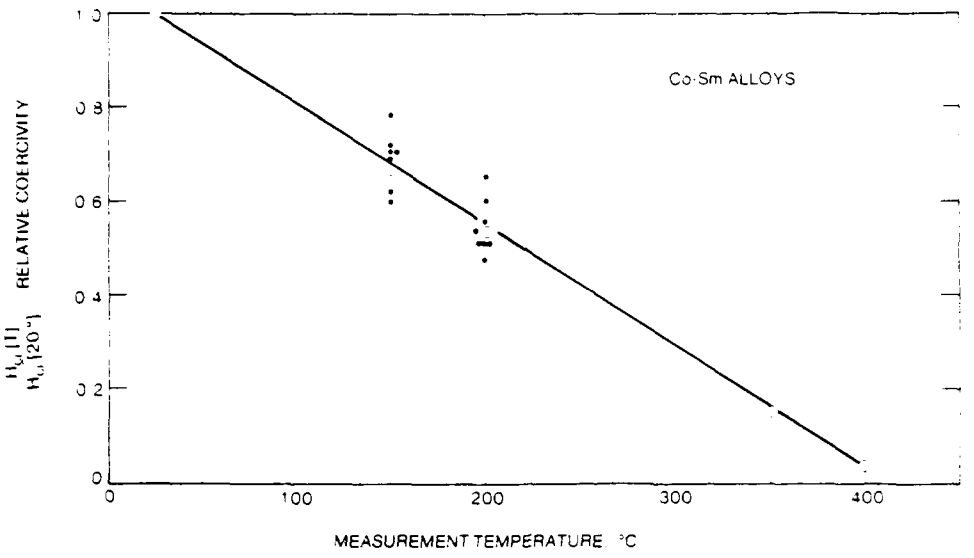

Figure 10. Variation of Coercive Force with Temperature

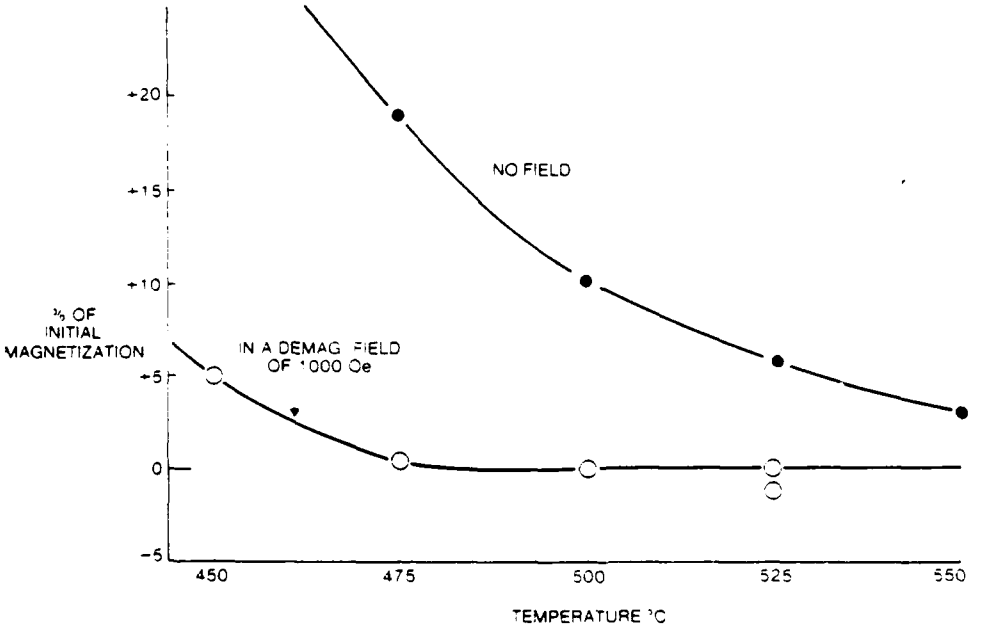

Figure 11. Magnet Demagnetization Versus Temperature

result in higher non-recoverable loss of magnetization after remagnetizing at room temperature (Figure 12). Thus, a thermal treatment below 500°C is preferred to a treatment above 500°C. The danger zone for metallurgical change is from 500°C to about 800°C. Above 850°C the magnet can, with proper care, be heat treated without a loss of properties.

The domain structure of a demagnetized magnet heated to 500°C, without a field, is shown in Figure 13A. It is very similar in appearance to a magnet thermally demagnetized at 900°C (Figure 7A), and consists of a uniform distribution of multidomains. Thermal demagnetization at 400°C is not as effective as 500°C (Figure 11) and the domain structure (Figure 13B) shows a large number of single domain grains.

On the basis of these preliminary results it was decided to try to optimize this thermal demagnetizing treatment. The 38 magnets were remagnetized after the 205°C studies and heated to a temperature in the range 425 to 480°C in a demagnetizing field of 1250 Oersteds.

The equipment consisted of two magnetizing coils surrounding the furnace. The magnet was heated to the desired temperature, held for about 30 minutes to be certain it was stabilized at this temperature, the demagnetizing field was applied for about 15 seconds, and the sample cooled to room temperature. The $4\pi J_o$ value was measured before and after the treatment. The results are listed in Table 7 and plotted in Figure 14. The goal was to reduce the magnetization below 5% of the initial magnetized level. This goal can be achieved by heating the magnet to a temperature in the range of 440 to 460°C and applying a -1250 Oersted field. The X-points in Figure 14 are the results obtained on the 16 Group A magnets to be used in Phase II. All except one were well below the 5% level set as a goal for the program.

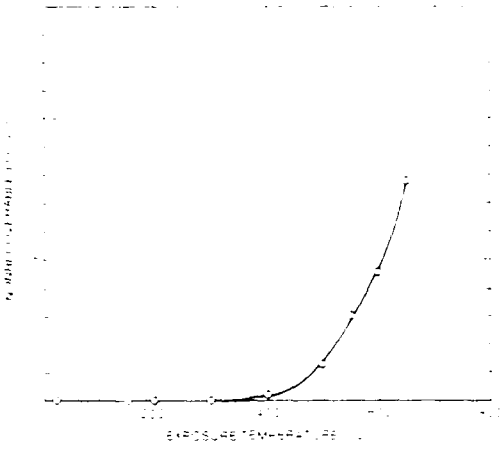

Figure 12. Nonrecoverable Loss Versus Exposure Temperature

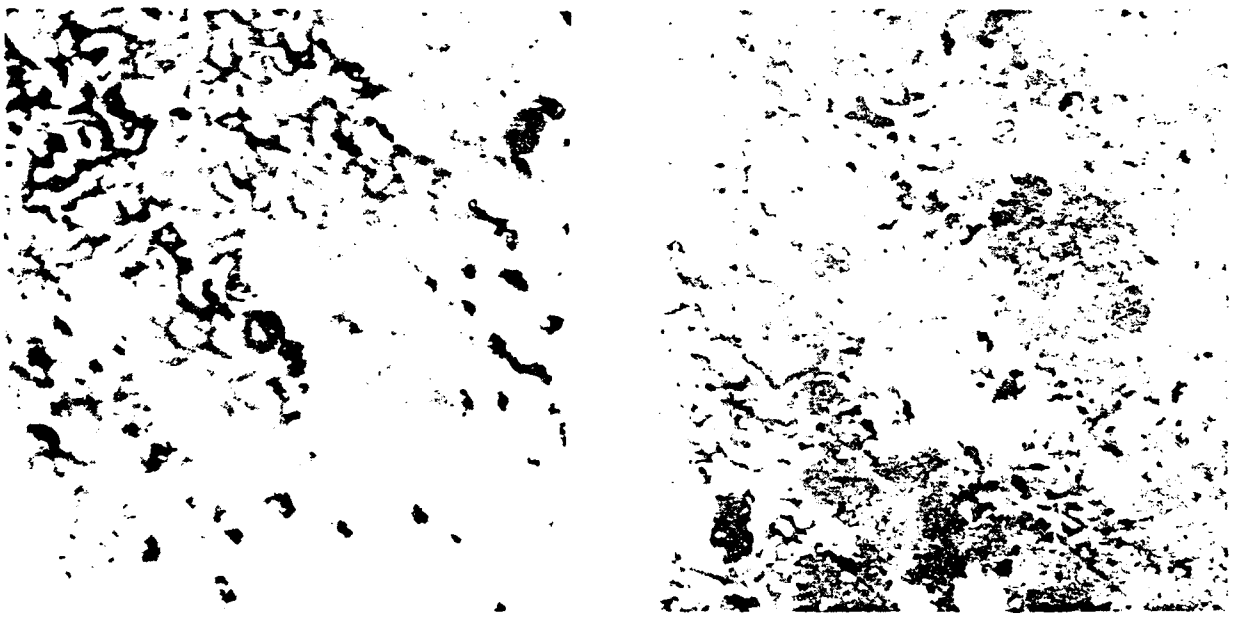

Figure 13. Magnet Domain Structure

TABLE 7

THERMAL DEMAGNETIZATION IN A 1250 OERSTED DEMAGNETIZING FIELD

	Temperature and % of Initial Value							
Group No.	°C	%	°C	%	°C	%	°C	%
12	465	-0.22						
14	455	-2.4	447	-2.2	437	-1.8	420	-0.8
A 18	443	+0.6						
33	455	-2.2	442	-0.9				
87	458	+0.6	419	+10.4				
112	425	+8.3	448	+1.2				
153	437	-0.7						
156	429	+7.3	447	+1.4				
A 157	442	+0.4						
158	431	+1.1	440	-1.3	444	-0.7		
159	434	+1.1	441	+1.1				
181	462	-1.9	439	+0.1	438	+0.8		
182	463	-1.3						
A 189	444	-0.6						
A 201	443	+1.8						
A 283	441	+5.4						
292	464	-0.7	446	+5.7				
294	467	-0.6	440	+5.5	440	+5.3		
301	455	-0.6						
A 303	442	-0.4						
A 310	442	+1.8						
315	469	-0.2	481	-2.3				
A 321	443	-0.1						
330	463	-2.4						
A 340	441	+2.3	+2.3					
343	453	-0.8	445	+0.4				
345	454	-0.5	440	+2.2				
A 346	454	-0.4	443	+2.7				
348	480	-0.4						
A 351	442	+1.6						
354	454	+1.0	433	+8.9				
A 358	441	-1.0						
A 367	442	+1.7						
371	453	-2.2						
380	453	-1.0	442	+0.8				
A 382	442	+2.4						
A 387	443	+1.9						

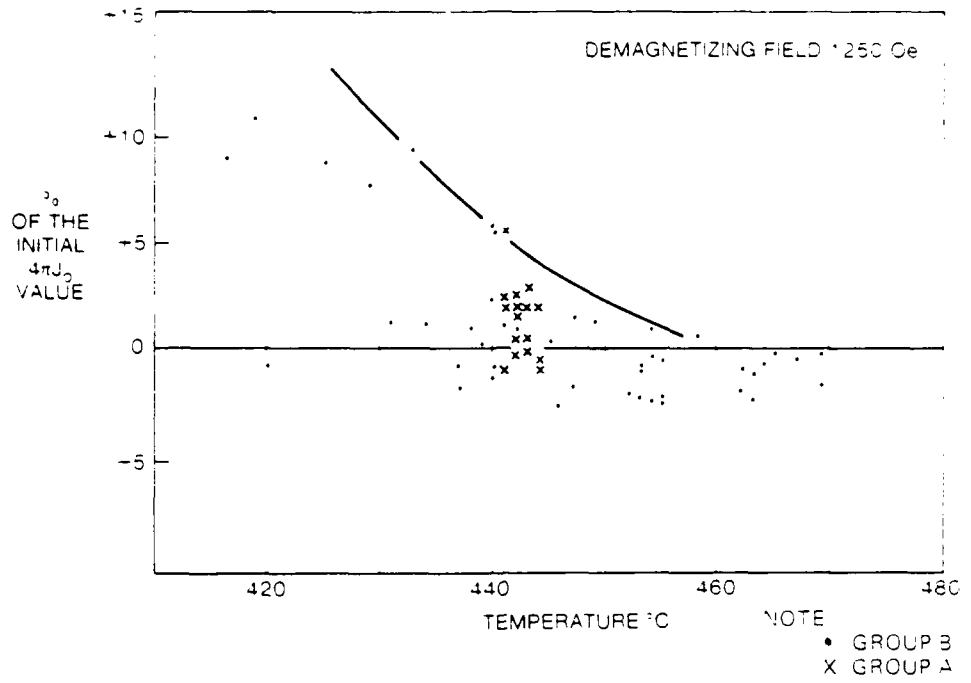

Figure 14. Thermal Demagnetization Results

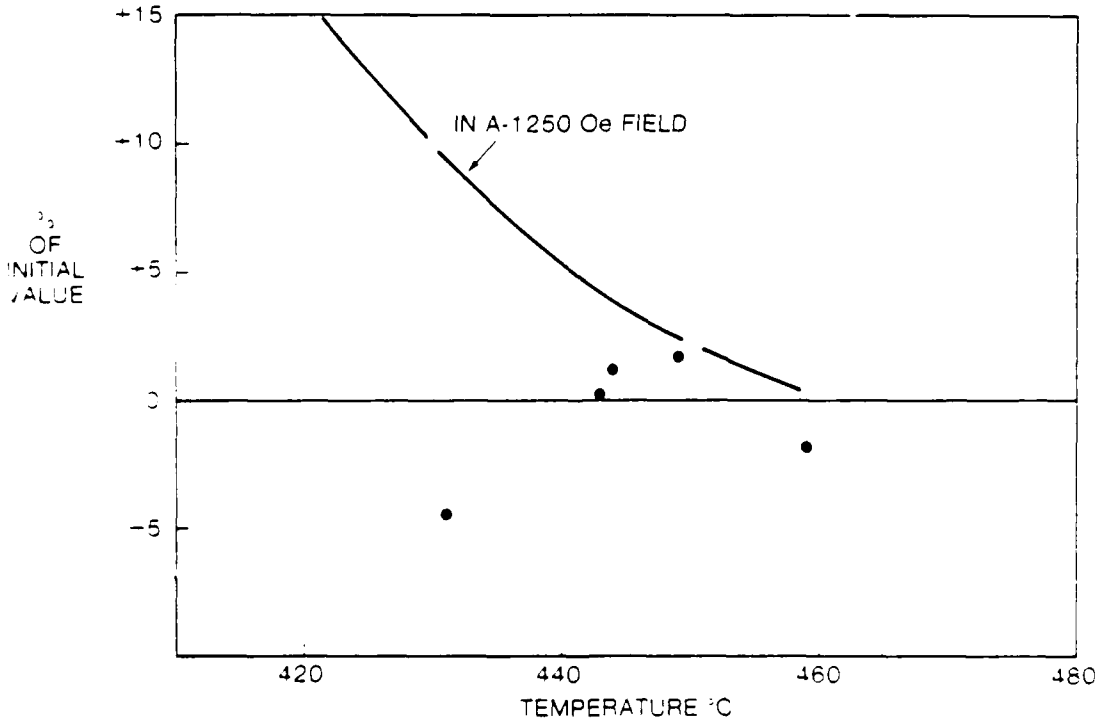

Figure 15. Thermal Demagnetization Results - Alternate Process

OTHER DEMAGNETIZING METHODS

After completion of the above additional studies have shown that other combinations of field and temperature are effective in reducing the magnetization to a low level. For example, exposing the magnet to a demagnetizing field greater than intrinsic coercive force at room temperature, followed by heating the magnet to a temperature in the 440-460°C range without a field resulted in $4\pi J_o$ levels equivalent to those demagnetized by a -1250 Oe field in the same temperature range. A comparison of the two methods is made in Figure 15, where it is shown that exposure to a high demagnetizing field prior to thermal treatment yields results comparable to those obtained when a field of -1250 Oe is applied at the thermal demagnetization temperature. The high field required to exceed the room temperature intrinsic coercive force is readily obtained by a pulse field generator.

Another method is to heat the sample first to about 450°C, remove it from the furnace, and quickly expose it to a decaying ac field of the order of 1000 Oersteds. For example, a magnetized magnet (No. 153) was first heated to 445°C, then it was removed from the furnace and while still hot exposed to an ac field of about 500 Oersteds. This treatment resulted in a magnetization level of +1.1% of the initial level compared to a value of -0.7% for the same magnet after exposing for a few seconds to a -1250 Oe field while at 437°C. This method shows promise and should be considered for production demagnetization of magnets. The same approach could be used with the dc demagnetizing field. The dc field generating equipment could be located near the furnace and the hot sample transferred to it.

(4) REMAGNETIZATION

It was agreed that the magnetizing field for the in-place magnetization fixture would be 25 kOe. This was a compromise as to what the fixture designer thought was attainable and what was thought to produce the maximum remagnetization of the magnet without saturating it. In the current study the magnetizing field was varied from 15 kOe to

60 kOe and its effect on B:H properties was studied. Sixteen magnets not selected for the Phase II program or the compression strength study were used. The remagnetization data for thermally demagnetized magnets are plotted in Figure 16. For these magnets, an applied field of about 27 kOe was needed to exceed all the specification values and a field of 60 kOe to equal the initial as-received values.

An applied field of 27 kOe corresponds to an internal field of about 24 kOe, because the demagnetizing field, H_o, of the open-circuit magnetic is about 3 kOe. That is,

$$H = H_{applied} - 3000$$

Figure 17 gives similar data for another magnet where an applied field of 25 kOe is sufficient to exceed all the specification values. Table 8 gives additional results on the properties of magnets remagnetized at 25 kOe applied field (22 kOe internal field). Nine of the sixteen magnets failed to meet the 20 MGOe specification for $(B:H)_{max}$, although seven of these were only slightly lower. Increase of the applied remagnetizing field to 30 kOe increases the $(B:H)_{max}$ about 2% so that some of the marginal magnets after 25 kOe magnetization are now acceptable. This is shown in Table 9 and Figure 18. In Figure 18, only one magnet failed the $(BH)_{max}$ test when magnetized at 30 kOe. It is clear from these results that it is important to have the remagnetizing field as high as possible, a few kilo-Oersteds higher field can make a big difference in the number of acceptable magnets.

(5) COMPRESSION STRENGTH OF THERMALLY DEMAGNETIZED MAGNETS

There was some concern that the thermally demagnetized magnets might suffer a loss of mechanical properties; therefore, the compression strength was measured. Mildrum and Iden[7] have reported a wide variation of compression strength parallel to the alignment direction from 35 to 90 kpsi for rare earth/cobalt magnets with an average of 43 kpsi. In the current study, the range for three magnets measured parallel to the alignment direction was 70 to 87 kpsi and the

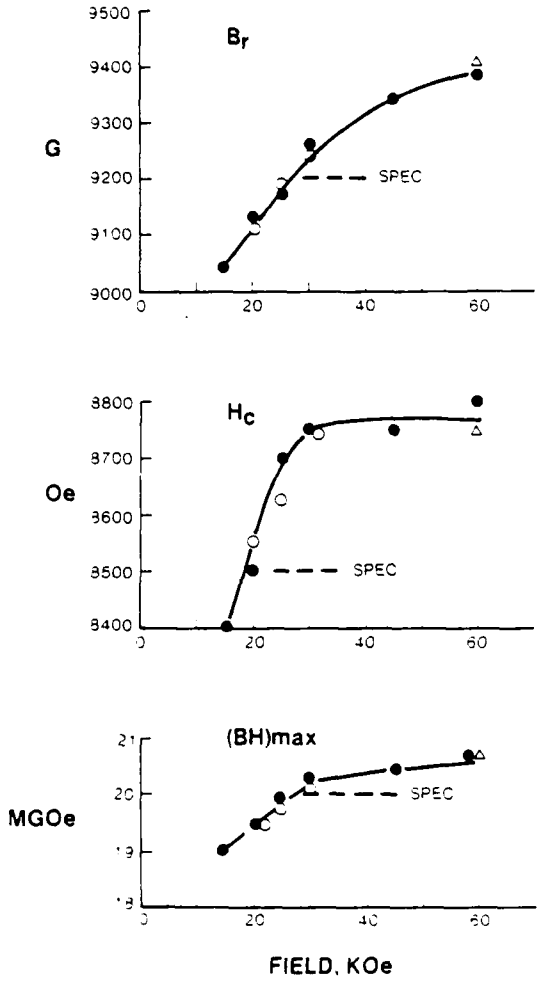

Figure 16. Effect of Remagnetizing Field on properties Magnet 158

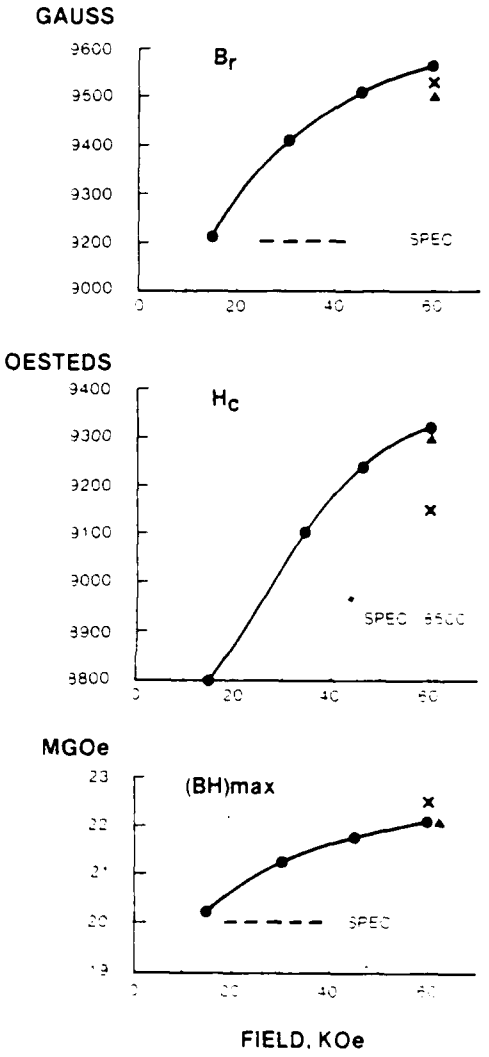

Figure 17. Effect of Remagnetizing Field on Properties Magnet 330

TABLE 8

REMAGNETIZATION OF THERMALLY DEMAGNETIZED MAGNETS

	B_r, KG			H_c, kOe			$(B:H)_{max}$, MGOe		
No.	Initial	After TD	%	Initial	After TD	%	Initial	After TD	%
12	9.4	9.1*	96	9.2	8.7	95	20.9	19.7*	94
14	9.5	9.3	99	8.9	8.5	96	21.0	19.9*	95
33	9.4	9.3	99	8.6	8.5	99	20.3	19.8*	98
112	9.2	9.0*	97	8.9	8.7	98	20.5	19.5*	95
153	9.5	9.5	100	9.0	9.1	101	21.3	21.6	101
156	9.3	9.0*	98	9.0	8.8	98	20.7	19.8*	96
158	9.5	9.2	97	8.8	8.6	99	20.7	19.8*	96
159	9.1*	9.0*	98	8.9	8.7	98	20.3	19.5*	96
181	9.3	9.2	99	9.0	8.8	98	21.0	20.3	97
330	9.5	9.4	99	9.3	9.1	98	22.1	21.4	97
343	9.5	9.3	98	9.2	8.9	97	21.7	20.7	95
345	9.3	9.1*	99	9.0	8.8	98	20.9	20.1	96
348	8.9*	8.5*	95	8.6	8.1*	94	19.1*	17.1*	90
354	9.1*	8.8*	97	8.9	8.5	96	20.3	18.8*	93
371	9.7	9.5	98	9.4	9.0	95	22.8	21.3	93
380	9.6	9.2	96	9.4	8.9	95	22.5	20.5	91
Mean	9.4	9.2	98	9.0	8.7	97	21.0	20.0	95

*Value below specification requirement.

TABLE 9

COMPARISON AS-RECEIVED MAGNETS WITH REMAGNETIZED MAGNETS

No.	As Received 60 kOe $4\pi J_o$ Gauss	$(B:H)_{max}$ MGOe	Thermodemag. 25 kOe $4\pi J_o$ Gauss	$(B:H)_{max}$ MGOe	Thermodemag. 30 kOe $4\pi J_o$ Gauss	$(B:H)_{max}$ MGOe
12	9180	20.9	8860	19.5	8980	20.2
14	9300	21.0	9040	19.8	--	--
33	9190	20.3	8930	19.8	--	--
87	9120	20.4	--	--	8970	20.0
112	9120	20.5	8830	19.5	--	--
153	9400	21.3	9330	21.6	--	--
156	9150	20.7	8900	19.8	--	--
158	9260	20.7	9040	19.9	9110	20.3
159	9060	20.3	8870	19.4	8890	19.8
181	9290	21.0	9100	20.1	9130	20.3
292	9000	20.3	--	--	8670	18.7
294	9040	20.4	--	--	8830	19.0
315	8970	19.7	--	--	8660	18.6
330	9480	22.1	--	--	9260	21.4
343	9410	21.7	9120	20.6	--	--
345	9190	20.9	8660	19.8	--	--
348	8790	19.1	--	--	8240	16.7
354	9040	20.3	8590	18.3	--	--
371	9590	22.8	9320	21.3	9400	21.7
380	9480	22.5	9030	20.1	--	--

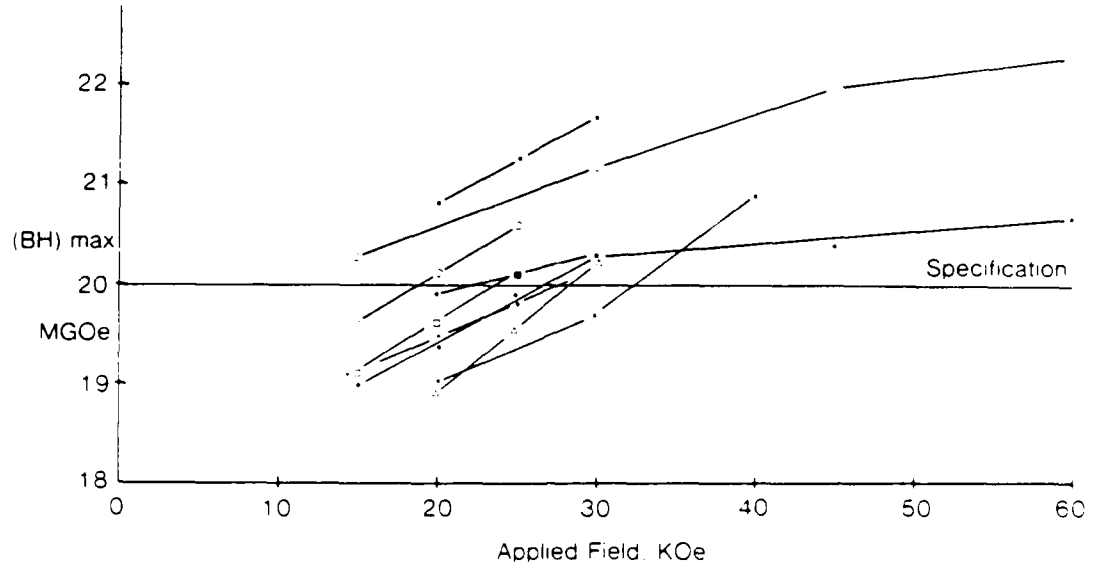

Figure 18. Remagnetization Curves for Thermal Demagnetized Magnets

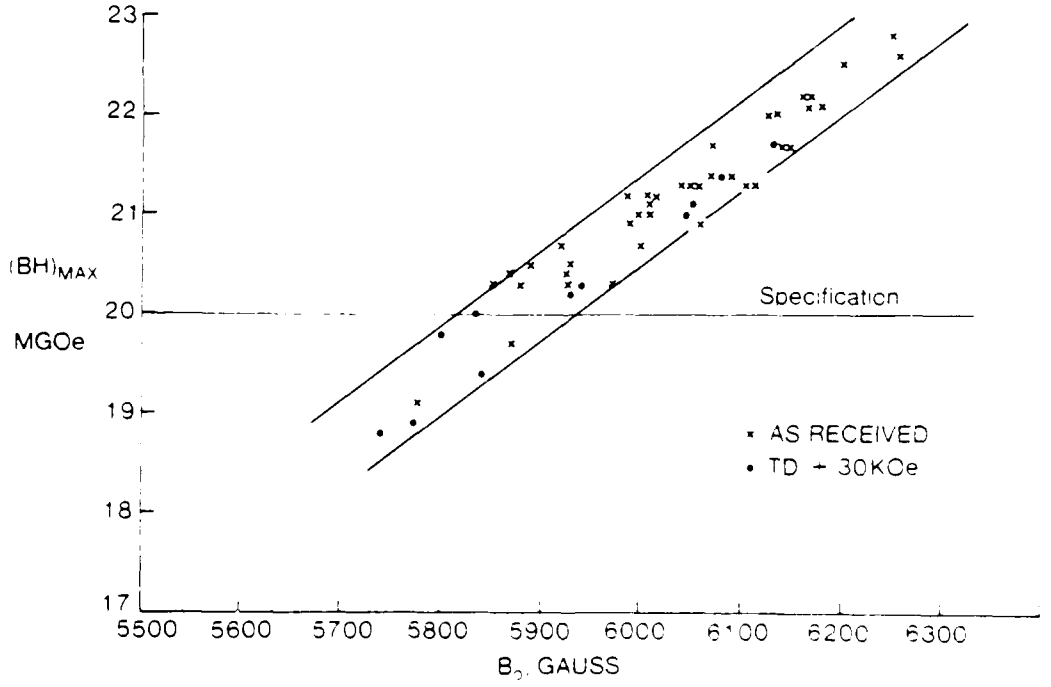

Figure 19. Comparison of Open Circuit Magnetization Values to Maximum Energy Product Specification

perpendicular measurement was 51 to 92 kpsi. Thus, there appears to be no indication of a loss of compression strength after thermal demagnetization in the 450°C temperature range, see Table 10.

b. Fixture Design

The contract required that a magnetization fixture and a measuring fixture capable of accepting a 150 kva rotor disc be designed under phase I effort.

(1) Remagnetization Fixture

A remagnetization fixture was designed to accept an unmagnetized 150 KVA rotor disc. The magnets located in the rotor disc assembly are to be magnetized in the circumferential direction with adjacent magnets repelling each other. Originally, this was to be accomplished by using a laminated multi-pole (14-pole) electromagnet device positioned around the rotor disc's outside diameter. The pole windings were constructed to be of alternate polarities. The electromagnetic device's pole lines up with the magnetic section of the shrink ring and in turn, the rotor disc pole pieces. The application of an electric pulse to the electromagnetic device field windings then sets up a magnetic field concentrated through the magnet, causing it to become magnetized.

Consultations were held with LDJ Electronics (Troy, Michigan) confirming magnetizer capabilities and the magnetization fixture design. The following concerns were factored into the fixture design:

- The detail design analysis method was considered impractical as the magnetic sections in the rotor (magnetic shrink ring section and pole piece) would be saturated and the magnet would have a variable permeability as it is being magnetized. A conservative approach was taken where the magnet sat in free space and the magnet had infinite permeability.

TABLE 10

COMPRESSION STRENGTH TEST RESULTS

	As Received				Thermal Demagnetization		Compression Data		
No.	B_r KG	H_c kOe	$(B:H)_{max}$ MGOe	$4\pi J_o$	Temp °C	% Initial	Direction	Load Pounds	kpsi
159	9.1	8.9	20.3	9.1	441	+1.1	‖	76600	82.5
181	9.3	9.0	21.0	9.3	438	+0.8	‖	80000	86.6
345	9.3	9.0	20.9	9.2	440	+2.2	‖	64800	70.3
343	9.5	9.2	21.7	9.4	445	+0.4	⊥	36000	50.9
380	9.6	9.4	22.5	9.5	442	+0.8	⊥	65000	91.9
292	9.0	9.0	20.3	9.0	446	+5.7	⊥	63000	89.2

Note: Mildrum and Iden, Goldschmidt informient 4/75, No. 35, Page 54 give data on compressive strength parallel to alignment: Range 35-90 kpsi and average of 42.7 kpsi.

- Simultaneous magnetization of the 14 poles was preferred.

- LDJ magnetizer, Model 6000CB, capable of 22,500 watt-seconds or 50,000 amps peak current would be capable of fulfilling the power supply requirements.

The fixture was designed to accept the 150 KVA rotor disc assembly (GE P/N 36C717474) with the inside diameter finished to accept the final rotor diameter dimension of 6.496/6.495 inches. A laminated stack height of 1.25 inches was employed to compensate for any misalignment. The fixture's inside diameter had a 0.007 inch air gap, to allow insertion of a 0.005 inch strip of polyimide sheet. This was used to prevent the magnetized disc from coming into direct contact with the magnetizing pole to simplify removal of the magnetized rotor disc.

The magnetization approach selected is similar to the one used in industry for the magnetization of control type Permanent Magnet Generators (PMG) with magnetizing fields similar to the proposal goal (25 kOe) for this program. The difference in the approach for this program lies in the direction of magnetization. Control type PMGs use Alnico type magnets, magnetized in the radial direction. The difference in magnet magnetization direction did not appear to be a significant problem.

The magnetization fixture features were as follows:

- Fixture designed to accept 150 KVA 14-pole rotor disc
- All magnets magnetized simultaneously
- Magnetization windings located on back iron and pole piece
- Back iron and pole piece winding in series
- Laminated iron - 0.020 inch thickness
- Mechanical ejectors to remove magnetized disc.

Based on an assumed leakage, the above fixture design (shown in Figure 20) was calculated to produce 25 kilo-oersteds through each pole with a magnetizing current of 30,000 amps. Space was provided in the

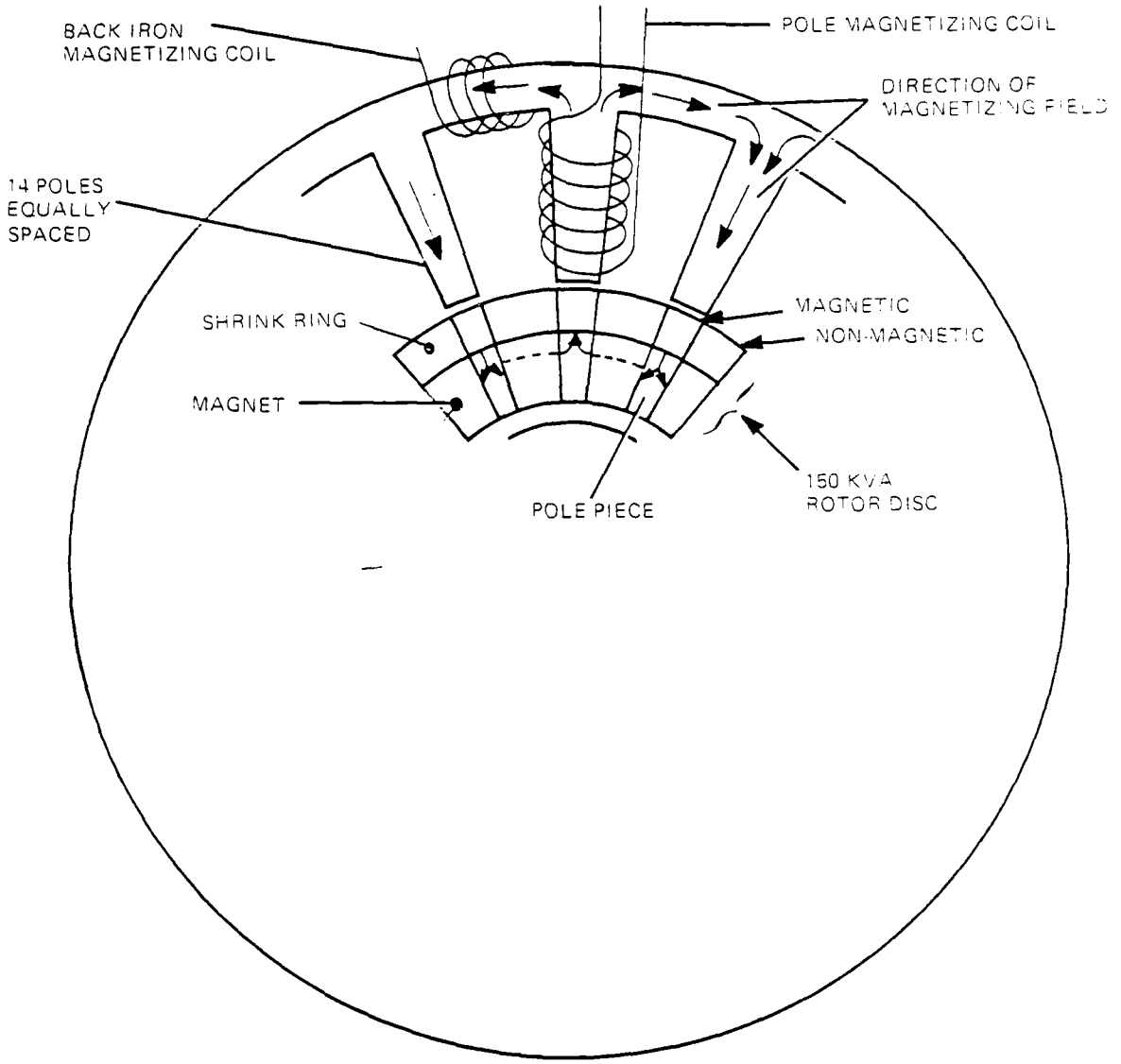

Figure 20. Magnetization Fixture - Original

fixture for additional series turns around the rotor disc if the magnetization fixture was marginal.

(2) Test Fixture

The specification required a fixture to be designed under Phase I to measure that radial magnetic flux density of each of the poles of a 150 KVA rotor disc. The fixture was required to simulate an actual stator winding and its associated air gap. Measurements of each pole was required to be accomplished by a pull coil and an integrating meter.

The above requirements were met by using surplus 150 KVA stator laminations. These stator laminations would be stacked together to give a 1.25-inch stack length to permit a 0.125-inch overhang on each end of the 1.0 inch thick rotor disc to minimize axial line-up inaccuracies with the test stator. The use of stator laminations would also satisfy the air-gap requirements. The test fixture stator would be wound with a balanced 9-phase winding similar to the 150 KVA stator. Thus the line-to-neutral voltage of any of the 9 phases would represent the average flux of the 14 poles when rotated. A thin, single turn, full pitch pull coil was selected to be positioned on the stator's inside diameter such that when connected to an integrating type fluxmeter, the individual pole magnetic flux could be measured for each of the 14 poles.

A stator support structure was designed to accept the above mentioned test stator to enable the test rotor disc to be driven by a variable speed DC motor. The drive shaft was designed to allow easy installation and removal of the test rotor disc, see Figure 21.

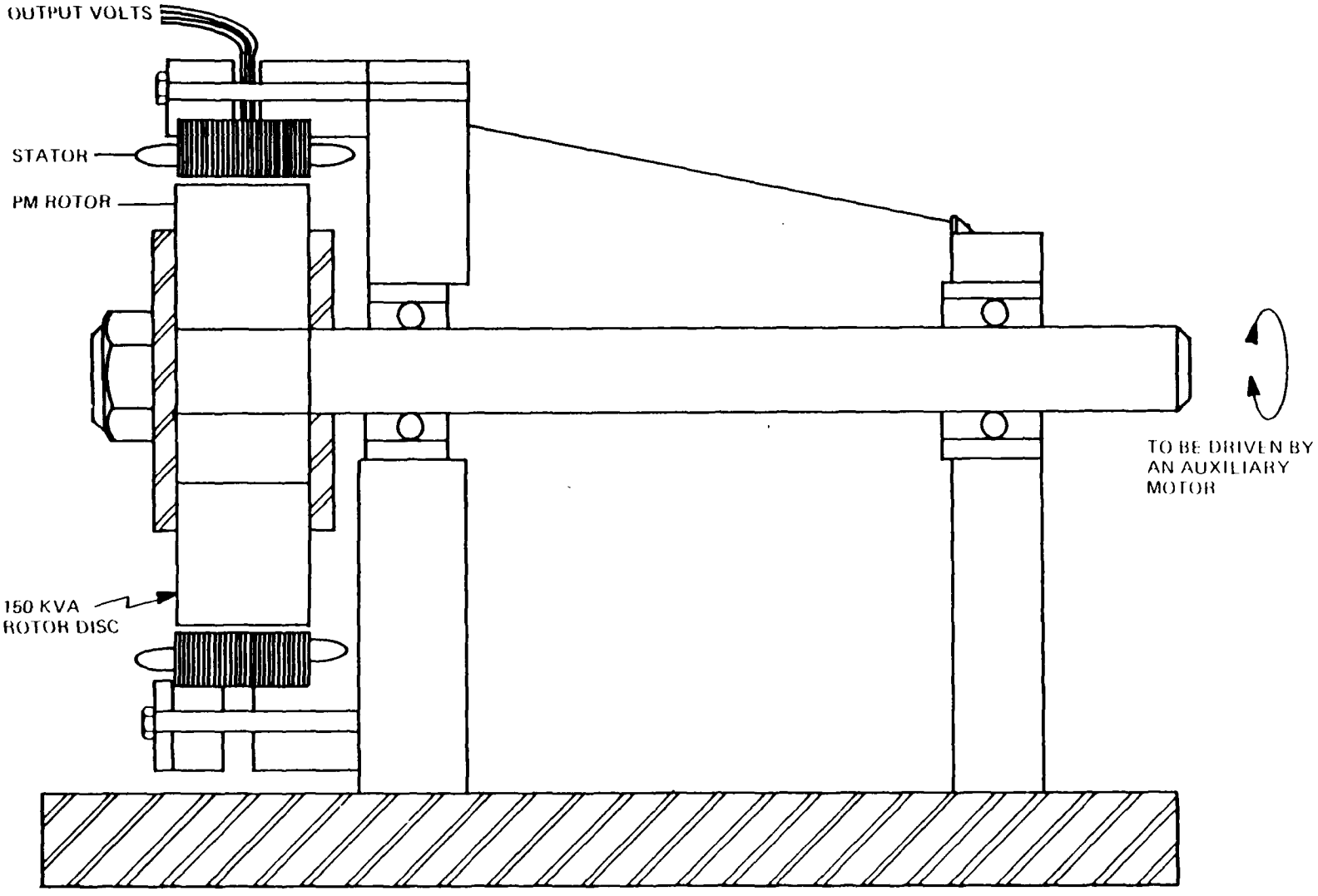

Figure 21. Test Fixture

3. PHASE II - FIXTURE FABRICATION/REMAGNETIZATION/TEST

a. Fixture Fabrication

(1) Magnetization Fixture - Original

Shown in Figure 22 is the magnetization fixture that was fabricated with the rotor disc installed. Figure 23 has the magnetizing fixture cover removed so the winding and interconnects can be viewed.

(2) Measurement Fixture

Shown in Figure 24 is the test fixture that was fabricated. The large leads are the 9-phase winding. The two small wires coming from the test stator are the pull coil connections. Figure 25 shows the 150 KVA rotor disc installed on the test fixture.

b. Disc Fabrication

The 16 magnets processed under Phase I of this program were assembled into a surplus 150 KVA pole and hub assembly and shrink ring. Care was taken to install the processed magnets in the identified polarity to assure they were remagnetized in their original polarity. A much larger magnetization level would be required to reverse the individual magnet's original magnet domain structure. It was also noted that the material fabrication process used on the original 150 KVA shrink ring produced random magnet and non-magnetic sections widths which did not align themselves closely with the magnet and pole interfaces.

c. Remagnetization and Test - Initial

The rotor disc assembled with magnetized magnets was tested using the test fixture shown in Figure 24. The results of the pull coil measurements are tabulated in Table 11. The generated L-N voltage of this rotor disc is shown in Table 12. The generated voltage waveshape produced by the search coil is shown in Figure 26 and produced by the stator winding shown in Figure 27.

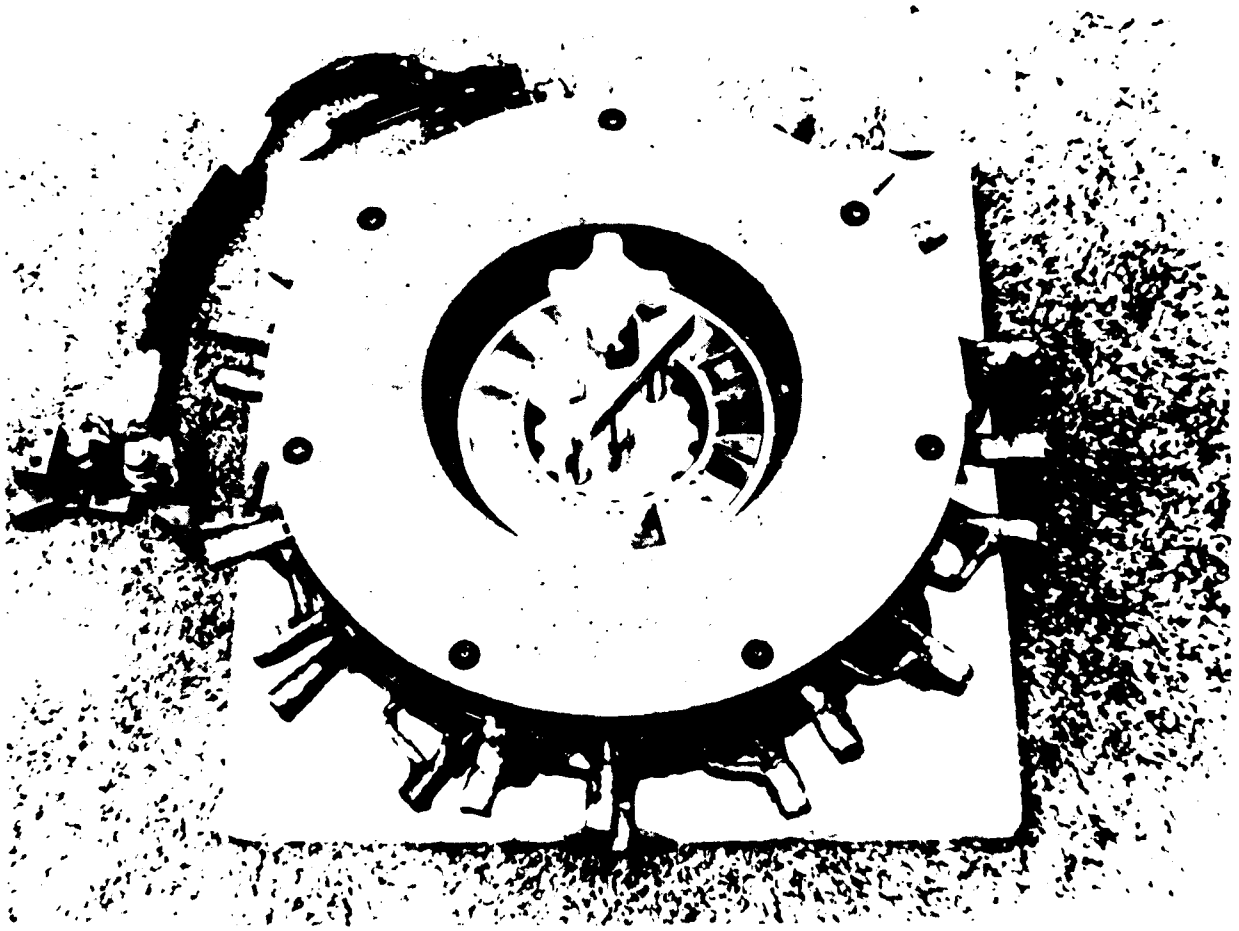

Figure 22. Magnetization Fixture

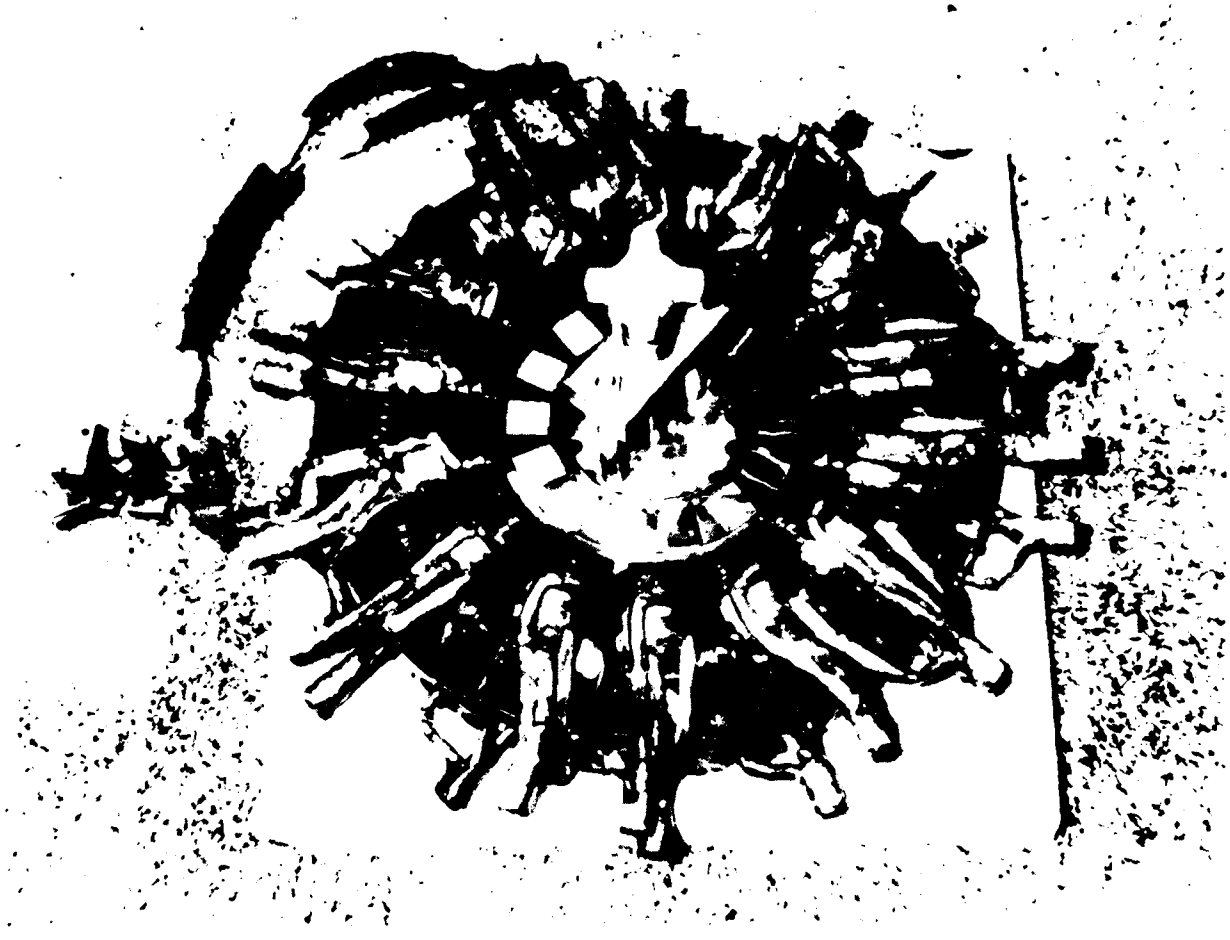

Figure 23. Magnetization Fixture (Original) - Winding and Interconnect

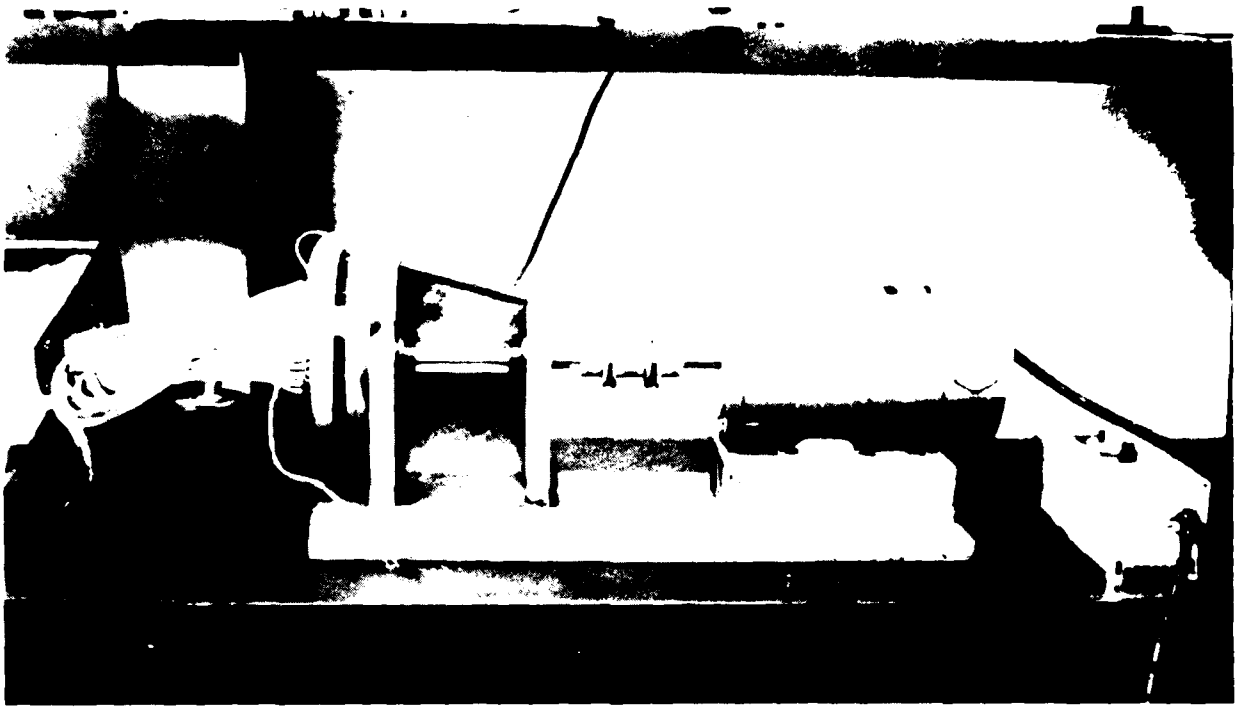

Figure 24. Rotor Disc Test Fixture

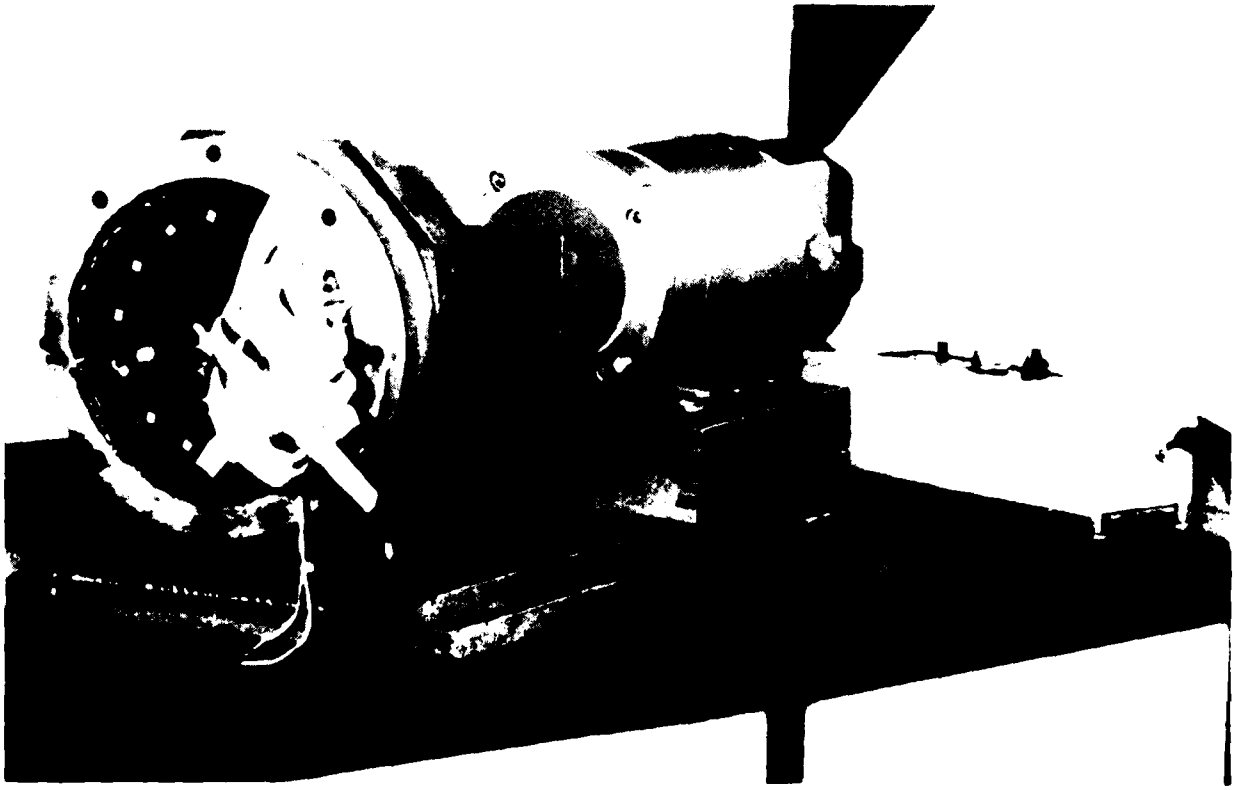

Figure 25. Test Fixture with Rotor Disc

TABLE 11

FLUX MEASUREMENT OF THE ROTOR DISC ASSEMBLED WITH MAGNETIZED MAGNETS

POLE NO.	FLUX METER READING IN VOLTS	FLUX PER POLE (FLUX METER CONSTANT 1V = 100K LINES)
1	1.065V	106,500 lines
2	1.068V	106,800 lines
3	1.057V	105,700 lines
4	1.063V	106,300 lines
5	1.066V	106,600 lines
6	1.067V	106,700 lines
7	1.081V	108,100 lines
8	1.094V	109,400 lines
9	1.084V	108,400 lines
10	1.085V	108,500 lines
11	1.073V	107,300 lines
12	1.081V	108,100 lines
13	1.076V	107,600 lines
14	1.077V	107,700 lines
Average	1.070V	

TABLE 12

GENERATED L-N VOLTAGE OF ROTOR DISC ASSEMBLED WITH MAGNETIZED MAGNETS

SHAFT SPEED	GENERATED VOLTAGE L-N	GENERATED VOLTAGE FREQUENCY
2132 RPM	4.48V	250 HZ
1066 RPM	2.24V	125 HZ

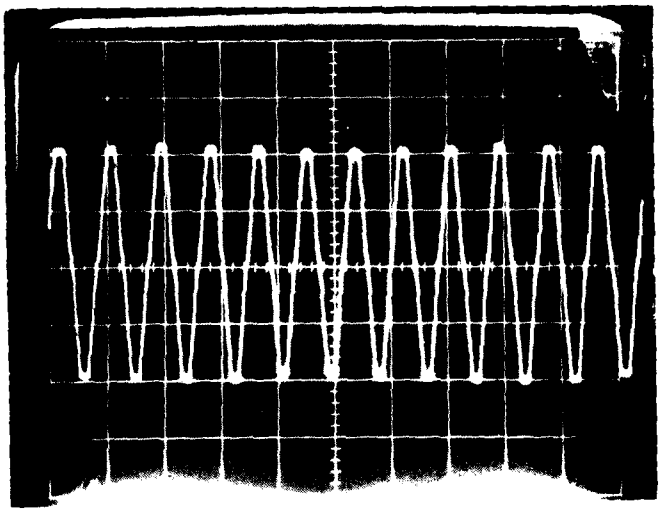

Figure 26. Generated Voltage Waveshape Search Coil - Rotor Disc Assembled with Magnetized Magnets

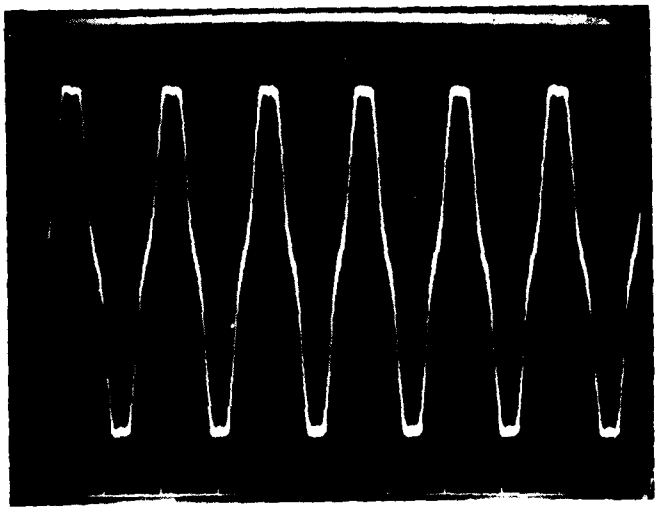

Figure 27. Generated Voltage Waveshape - Stator Winding L-N Rotor Disc Assembled with Magnetized Magnets

The rotor disc assembled with the demagnetized magnets processed in Phase I was positioned in the magnetization fixture (Figure 22). The winding connections were verified with a small DC field applied prior to connection to the LDJ Electronics 22,500 watt-second magnetizer to assure proper polarity magnetization. A DC current shunt was installed in the setup to measure the magnetization current applied. See Figure 28 which shows magnetization setup.

The application of the magnetization current was varied in four steps up to the total power supply capability after which the disc was removed from the magnetization fixture and measured in a similar manner as accomplished on the rotor disc assembled with magnetized magnets.

This initial magnetization attempt was only partially successful. See Table 13 for flux measurements. The magnetized disc was found to have attained a level of magnetization corresponding to approximately 37.7% of the values shown in Table 12.

The above test results indicated two areas limiting the success of this magnetization. The first area is the magnetizer. The magnetizer used was provided by a vendor (LDJ) who specializes in magnetics of large capacity, especially for rare earth/cobalt permanent magnets. A magnetizer with higher current capacity is made by this vendor but is a special order. The use of this larger magnetizer would increase the magnetization field but extrapolation from the results obtained indicates that this change would not do the complete job. The second area is the magnetizer winding. It is evident that the back iron turns were not effective. Provisions for laced turns around the magnet were included in the fixture design. The next step was to disconnect the back iron turns and incorporate the lace turns to evaluate their effectiveness.

Shown in Figure 29 is the magnetization fixture with lace turns incorporated. Various combinations of wiring; series, parallel, one-pole, were tried to increase the magnetization current level and/or

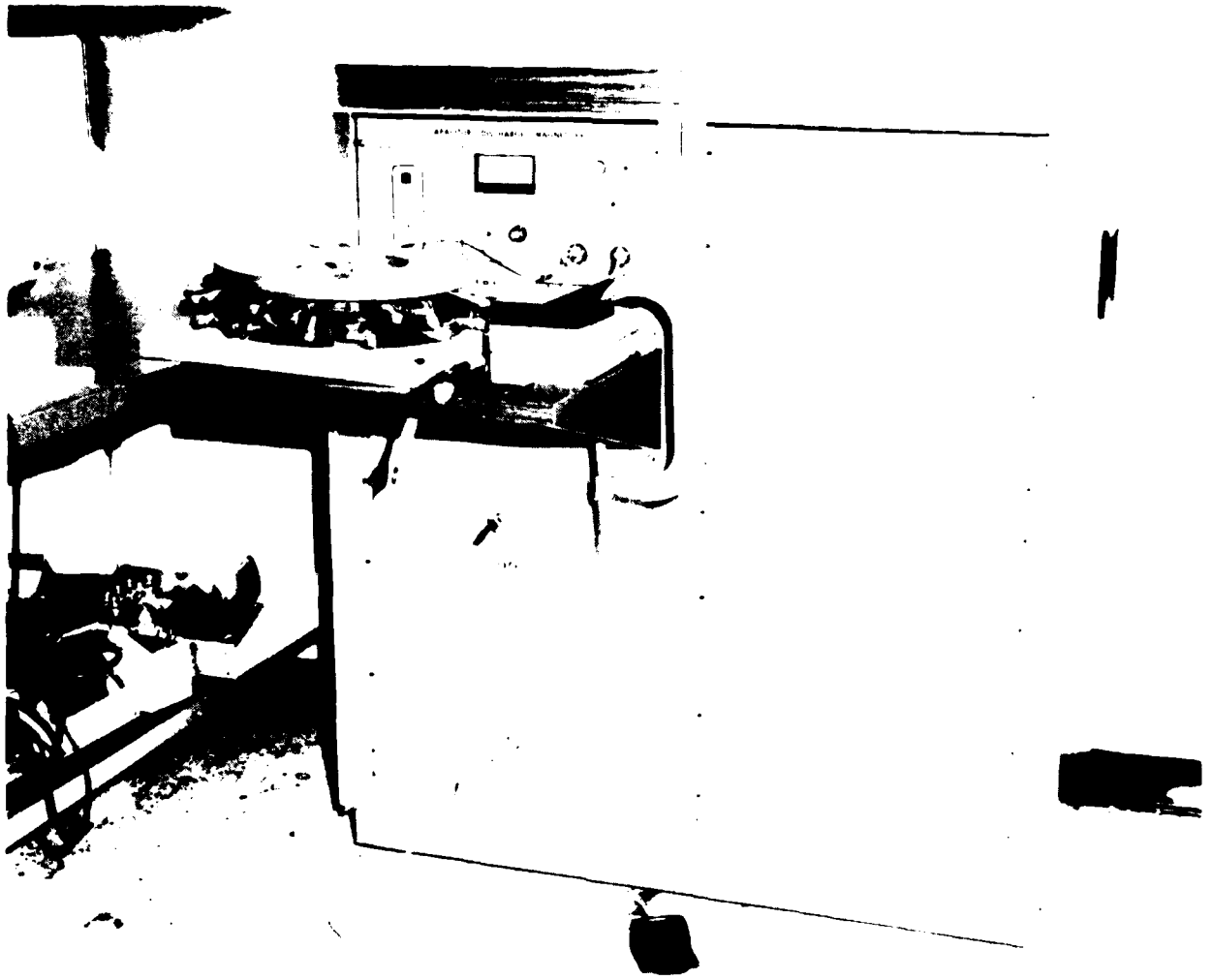

Figure 28, Magnetization Setup - Original

TABLE 13

FLUX MEASUREMENTS OF ROTOR DISC AFTER INITIAL MAGNETIZATION

POLE NO.	FLUX METER READING mVOLTS	% RECOVER
1	-356	33.3
2	+384	35.9
3	-235	22.0
4	+409	38.2
5	-280	26.2
6	+435	40.7
7	-280	26.2
8	+290	27.1
9	-215	20.1
10	+680	63.6
11	-745	69.6
12	+715	66.8
13	-260	24.3
14	+360	33.6

Average 37.77

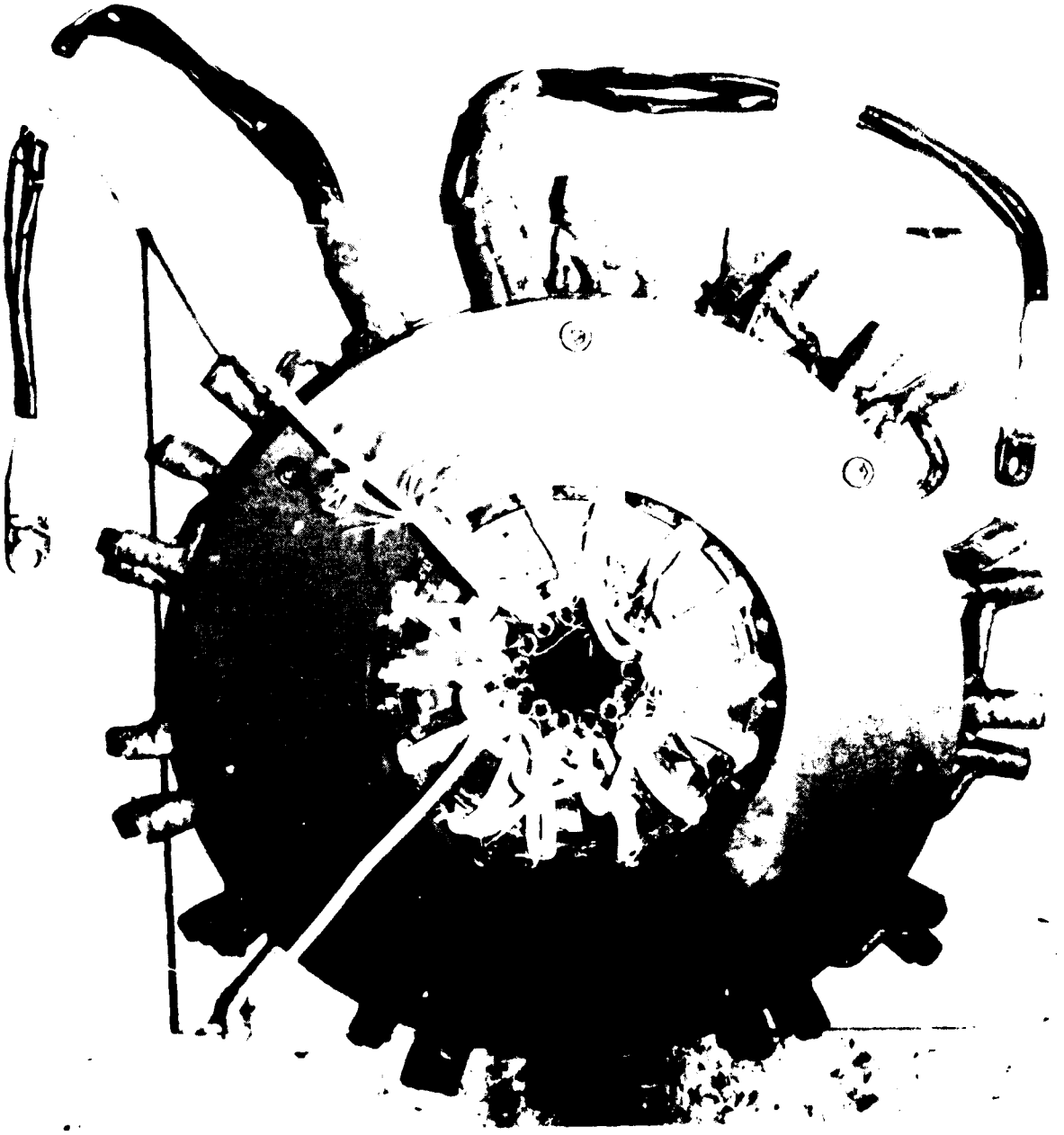

Figure 25. Magnetization Fixture with Supplemental Yoke

increase the number of magnetization turns for this fixture's configuration. The resulting measured level of magnetization did not change significantly from the original results. A review of the magnetization results with Dr. E. Richter and Dr. L. Martin concluded that two dimensional electromagnetic Finite Element Analysis (FEA) should be tried to obtain insight into the magnetization problem being experienced. The FEA program was developed by Corporate Research and Development Center and was not available at the start of this program.

d. Finite Element Analysis

This section discusses the results from a finite element magnetic field study of the magnetization arrangement for a 150 KVA rotor disc. The final conductor configuration is shown for the magnetization fixture, and the results of a non-linear finite element analysis are presented. By using these results to establish remanent magnetization levels in the permanent magnet material, it is found that the lack of magnetization of some parts of the magnet does not seriously affect the flux density in the air gap. The limitations of the analysis are discussed in light of the engineering judgements which must be made.

(1) Magnetization Arrangement

Figure 30 shows the arrangement of rotor, conductors, and back iron which form the magnetization structure. The permanent magnets are arranged in a "flux squeezing" manner in order to achieve higher air gap flux densities than would be possible from surface-mounted magnets. The magnetizing conductors are dimensioned 0.07"x0.14" and they are arranged in groups of three to obtain the needed amp-turn capability.

During the magnetization process a flux density of >2.4 Tesla is required in the preferred direction of magnetization in order to fully "charge" the magnet. It was found during earlier numerical studies that by placing the exciting coil sections over the ferromagnetic pole pieces rather than over the magnet, one could achieve a relatively

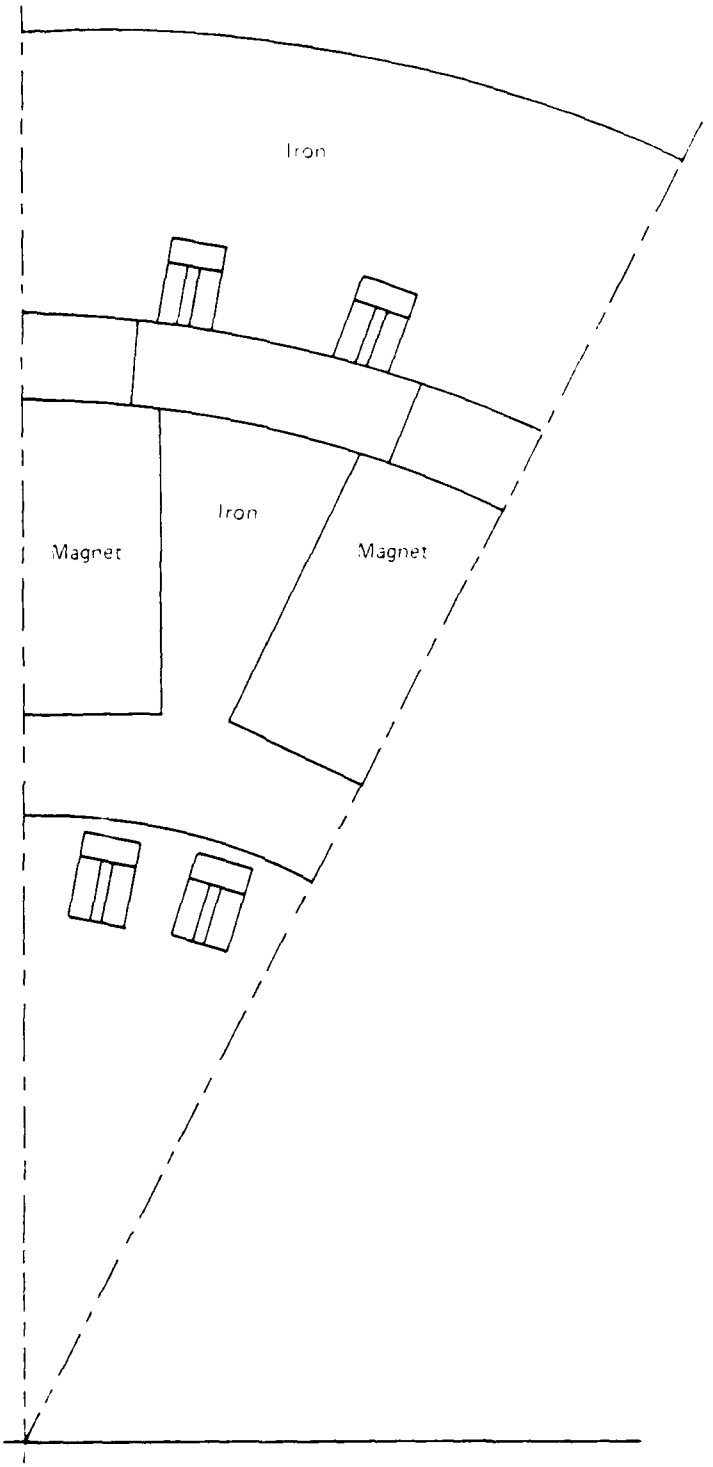

Figure 30. Rotor, Inductor and Back Iron Arrangement for Finite Element Analysis

uniform flux density throughout the magnet. The configuration in Figure 30 is the result of these experiences.

Because of the rather large conductor current density (4×10^3 A/in^2), much of the ferromagnetic iron is driven into heavy saturation. It was found that although the back iron structure is indeed saturated near the conductors, iron further away does help reduce the magnetization requirements somewhat, and is therefore included in the configuration.

(2) Finite Element Model

Because the radial centerlines of the magnet and the ferromagnetic pole pieces are lines of symmetry, only one-half pole pitch need be represented for magnetic analysis. An outline of the model is shown in Figure 31, while the division of the model into triangular finite elements is shown in Figure 32. This grid was produced using an automatic grid generator originally developed for homopolar inductor alternator analysis, with suitable modifications to allow for placement of currents.

The rare earth/cobalt magnet was represented magnetically by an air space, recognizing that its permeability relative to air is near unity. The ferromagnetic regions are given magnetic characteristics similar to M-19 magnetic steel. The conductor regions have unity relative permeability and carry current at a density of 4×10^3 A/in^2. Figure 33 shows the triangular decomposition of the air space region only so that one can see the placement of the conductors.

The nonlinear finite element solution program uses the vector potential solution method. The solution iterations are obtained by a matrix Newton-Raphson algorithm, and convergence is obtained when the relative change in the solution from one iteration to the next is less than one part in 10^5. The problem boundary conditions are set so that the magnetic radial centerline and the outer radius are (effectively)

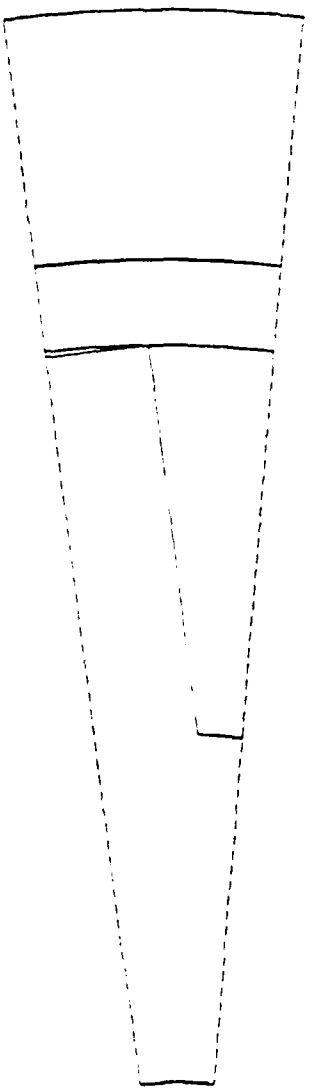

Figure 31. Outline Drawing for Finite Element Magnetic Field Model

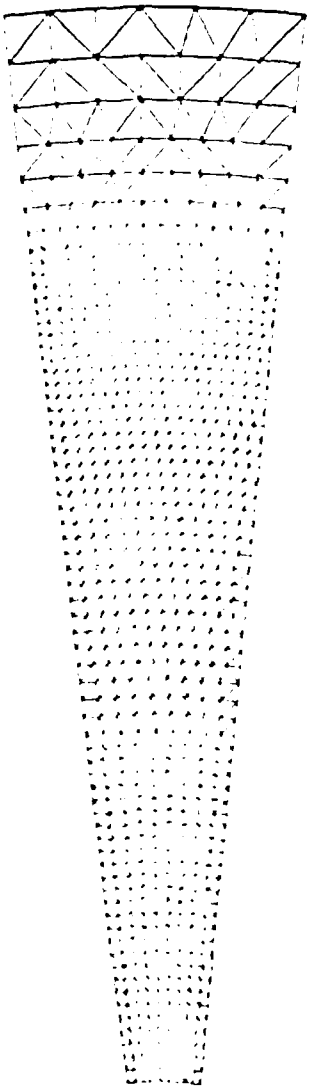

Figure 32. Triangular Element Discretization for Finite Element Model

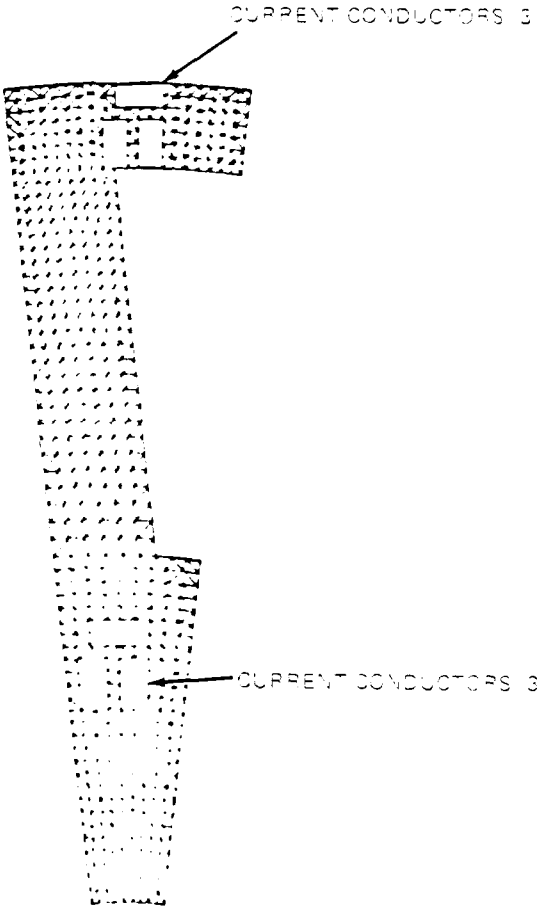

Figure 33. Triangular Element Discretization for Air Space Region Only

infinitely permeable boundaries, while the pole piece radial centerline and the inner radius form a flux line (constant vector potential) boundary. These conditions were thought to represent the problem at hand fairly well.

The results of the finite element analysis are shown in Figures 34-39. Figure 34 shows a qualitative picture of the magnetic field under magnetizing conditions; in two dimensions, the lines of constant vector potential represent magnetic field lines. One can see that within the magnet the field is relatively uniform, except near the lower right hand corner. By moving the conductors at the outer radius to a position over the pole piece iron, one effectively forces the flux further down into the iron, thereby producing a much more uniform field over the magnet length.

In order to get a more quantitative idea of the flux density in the magnet, the x-directed (preferred direction) flux density is sampled along the four lines depicted in Figure 35. Figures 36-39 show that nearly everywhere within the magnet the flux density exceeds the necessary 2.4 Tesla, with the exception of the lower right hand corner; this was expected from the flux plot.

Because much of the iron is operating at, or near, its magnetic saturation limit, it is felt that for small excursions about the chosen current density, the flux density should scale linearly with the current density.

(3) The Effect of Magnetization Uniformity on Magnet Performance

The one remaining question was how the non-uniformity of magnetization affects the magnet performance, particularly in regard to the corner problem. In order to answer this question, a finite element permanent magnet representation was used. This program currently only handles linear magnetic materials, but it was felt that the results accurately reflect what is happening in the air gap of the machine.

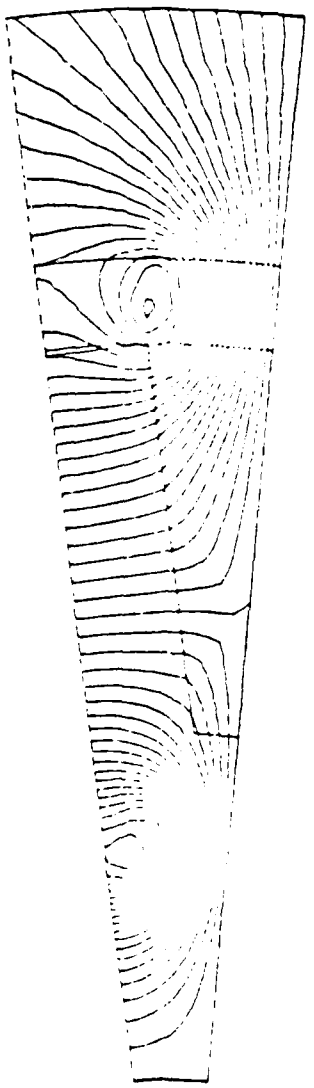

Figure 34. Flux Line Plot at Full Magnetization Current

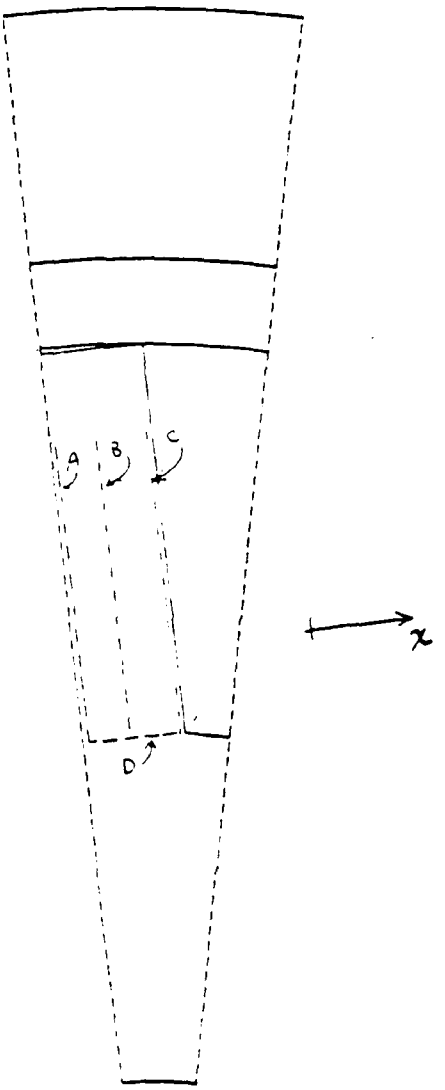

Figure 35. Flux Sampling Definition

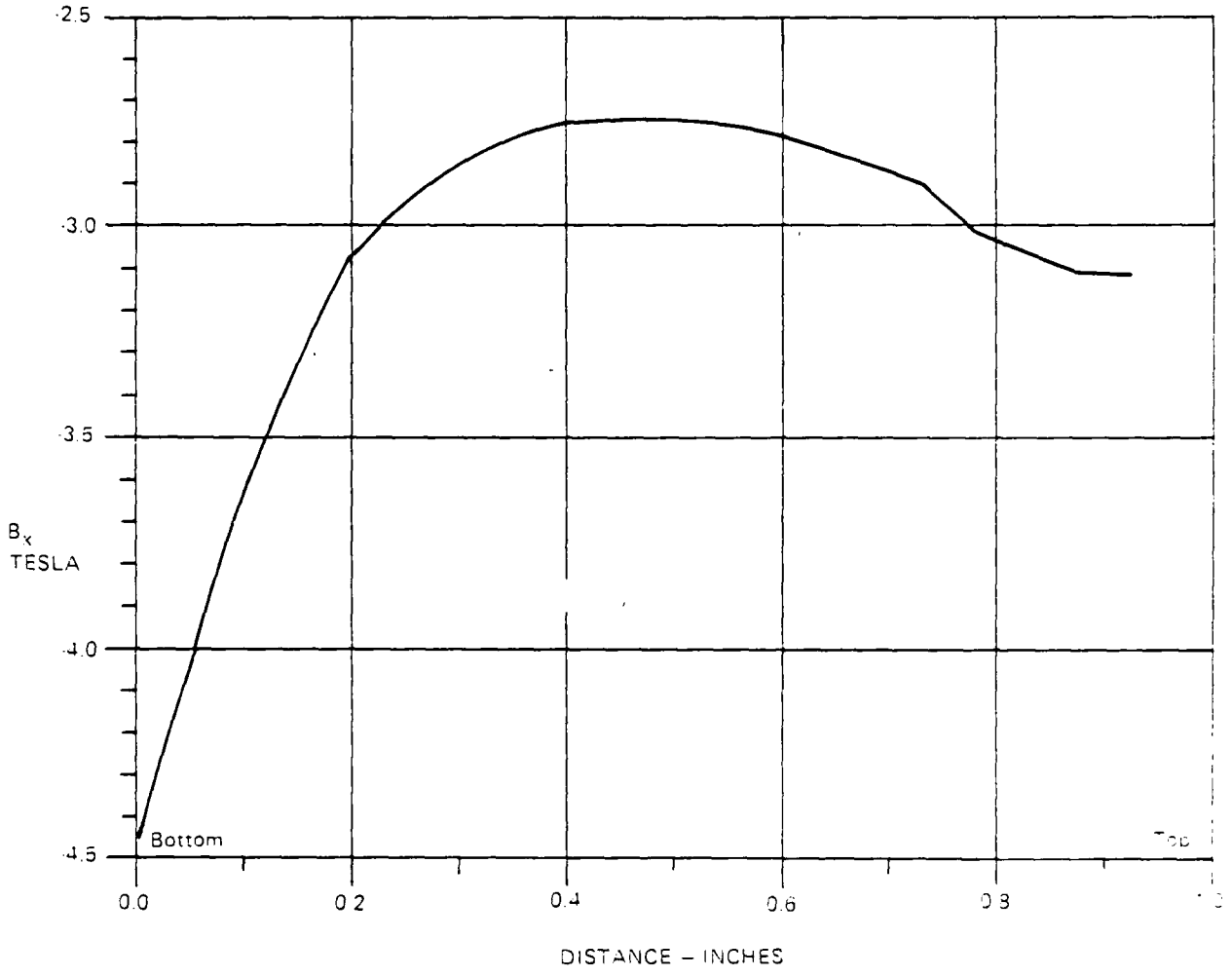

Figure 36. B_x Along Line A

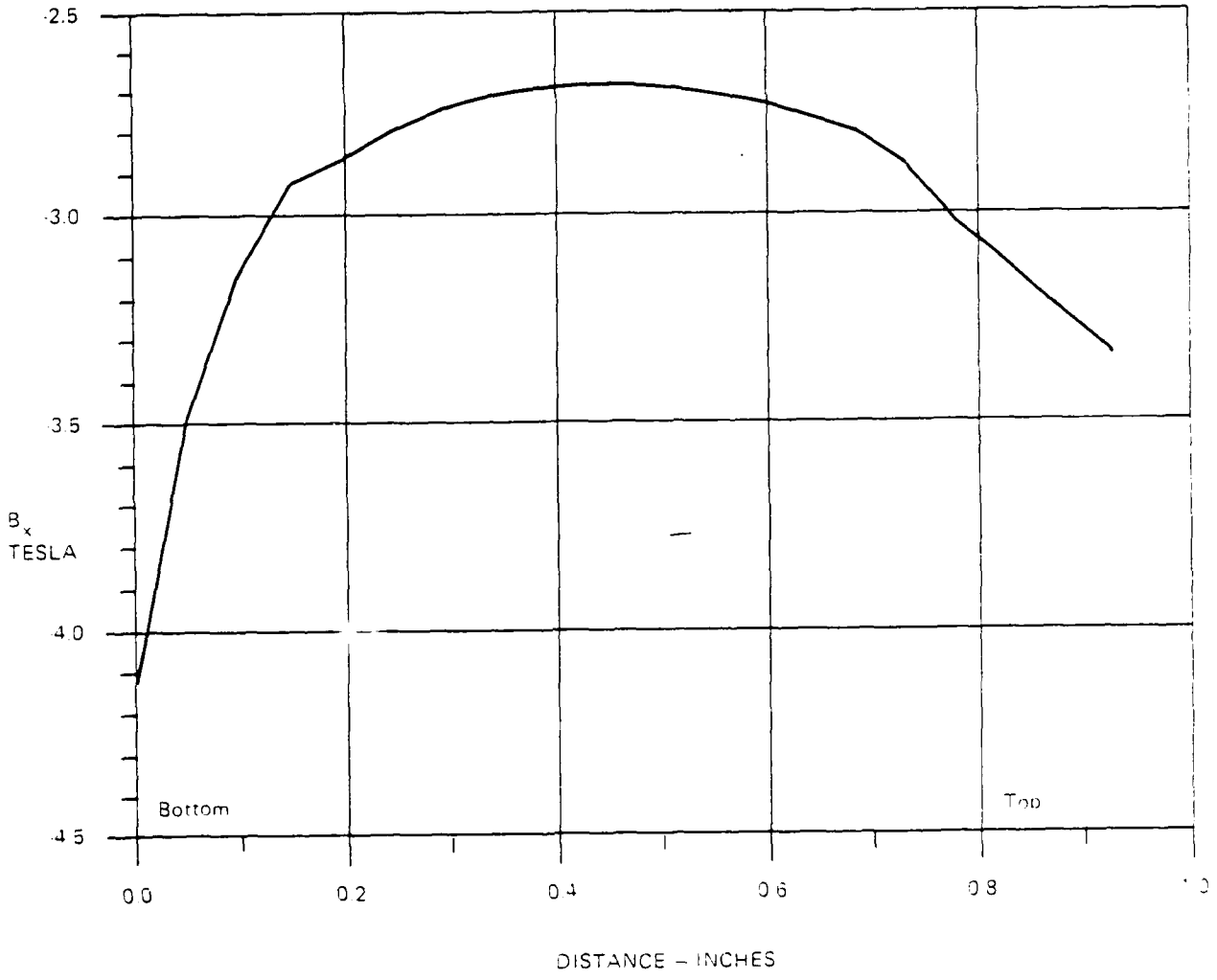

Figure 07. B_x Along Line B

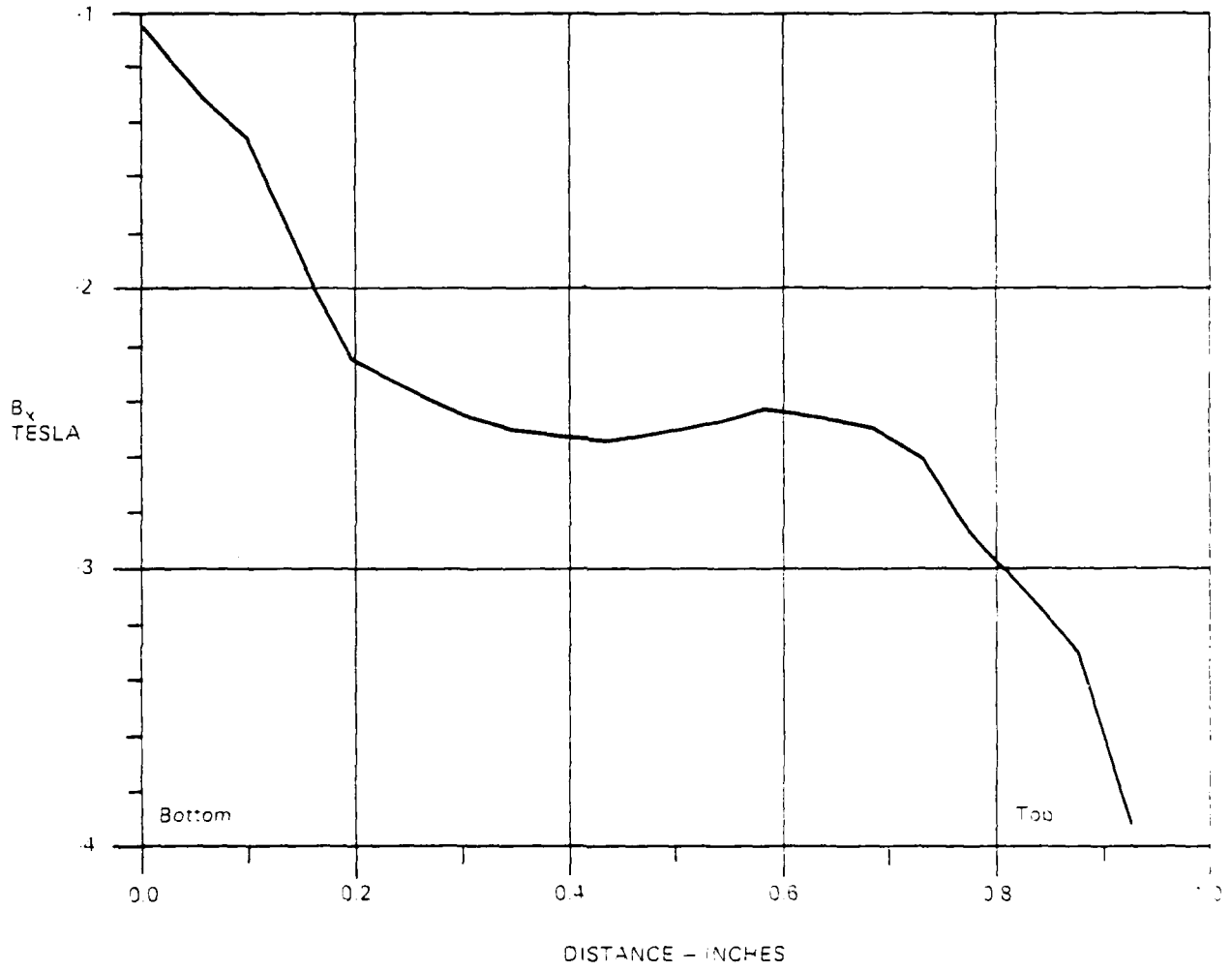

Figure 38. B_x Along Line C

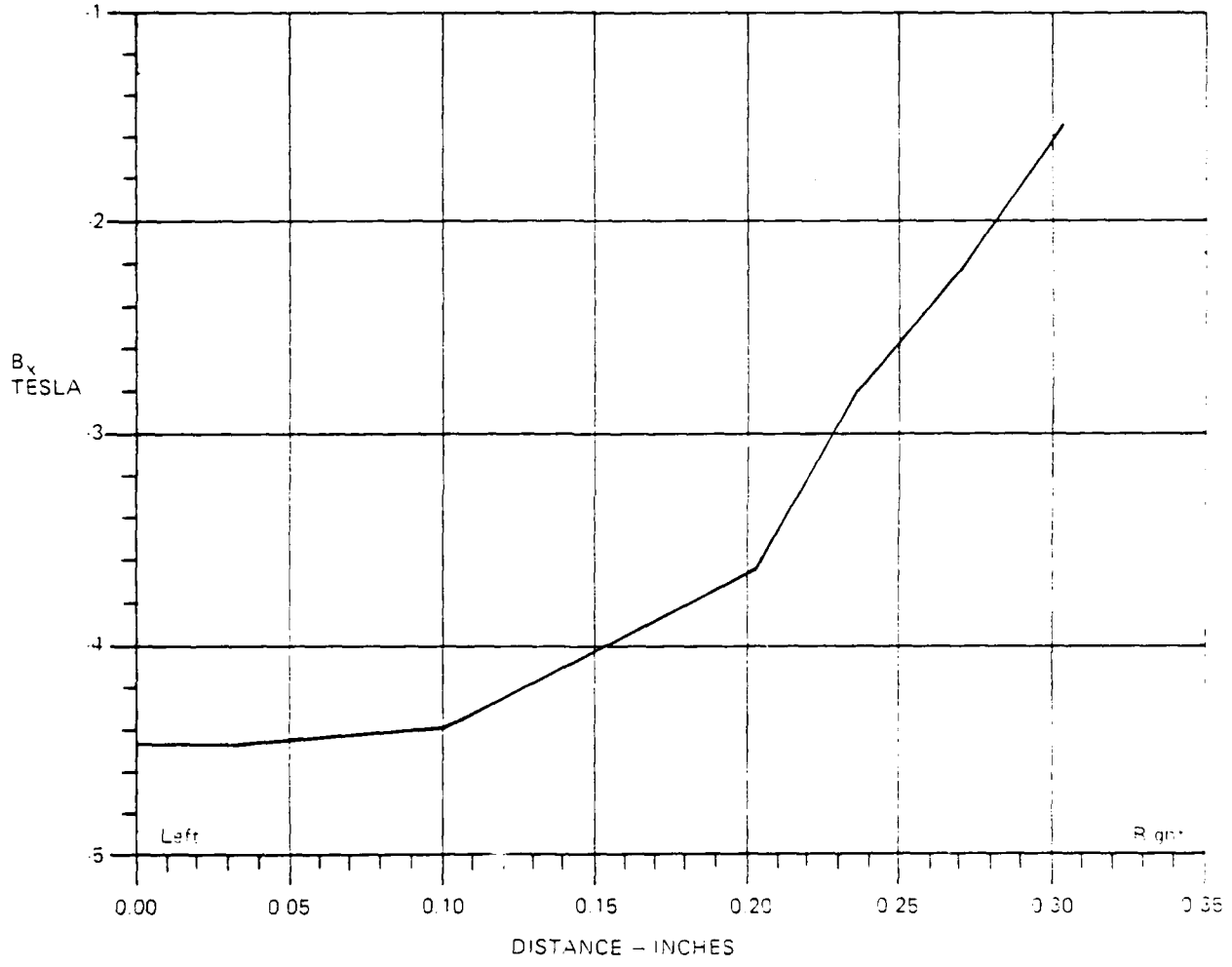

Figure 39. B_x Along Line D

A new finite element grid was generated which represented the same machine but with a smaller air gap (0.015"). The first test case assigned a uniform x-direction magnetization (0.8 μ_o) to the magnet material: the resulting flux plot is shown in Figure 40. The radial magnetic flux density on the stator side of the air gap is shown in Figure 41. This can be considered the ideal case, since the magnet is uniformly magnetized.

A second test case was configured to try to account for the non-uniform magnetization found earlier. The results of the magnetization calculations were used to assign a magnetization to each finite element of magnet material according to the following functional relationship:

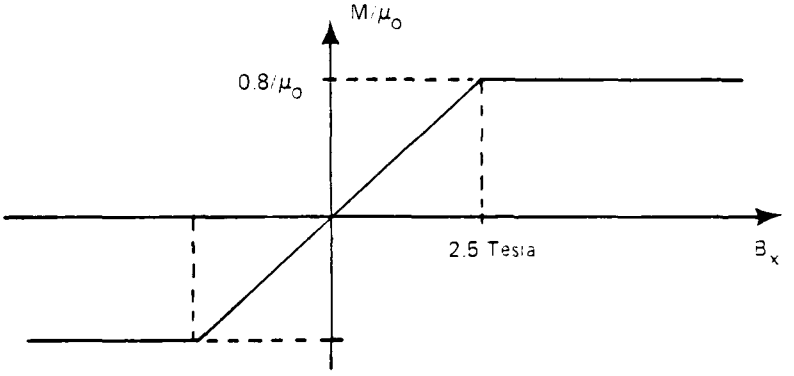

The resulting flux plot is shown in Figure 42; things do not appear to be much different from Figure 40, the uniform case. More quantitative information is provided by the radial magnetic flux density at the stator: Figure 43 shows that it is only a fraction smaller than that provided by the uniformly magnetized magnet.

These results indicate that the non-uniformity in the corner of the magnet will have little effect on the overall performance.

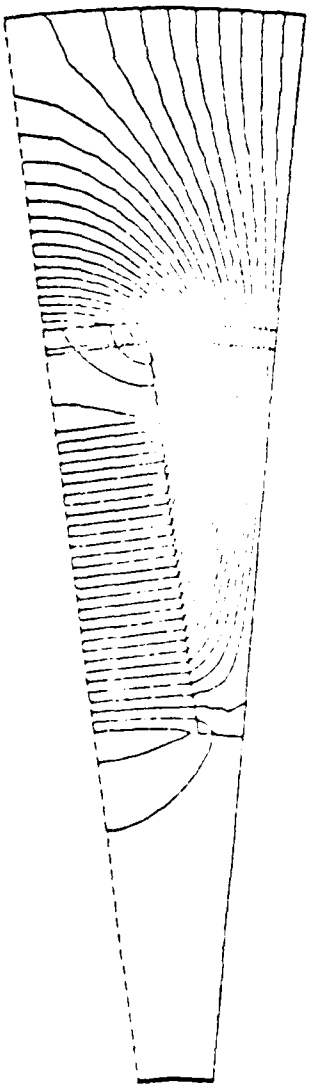

Figure 40. Flux Line Plot for Uniformly Magnetized Magnet

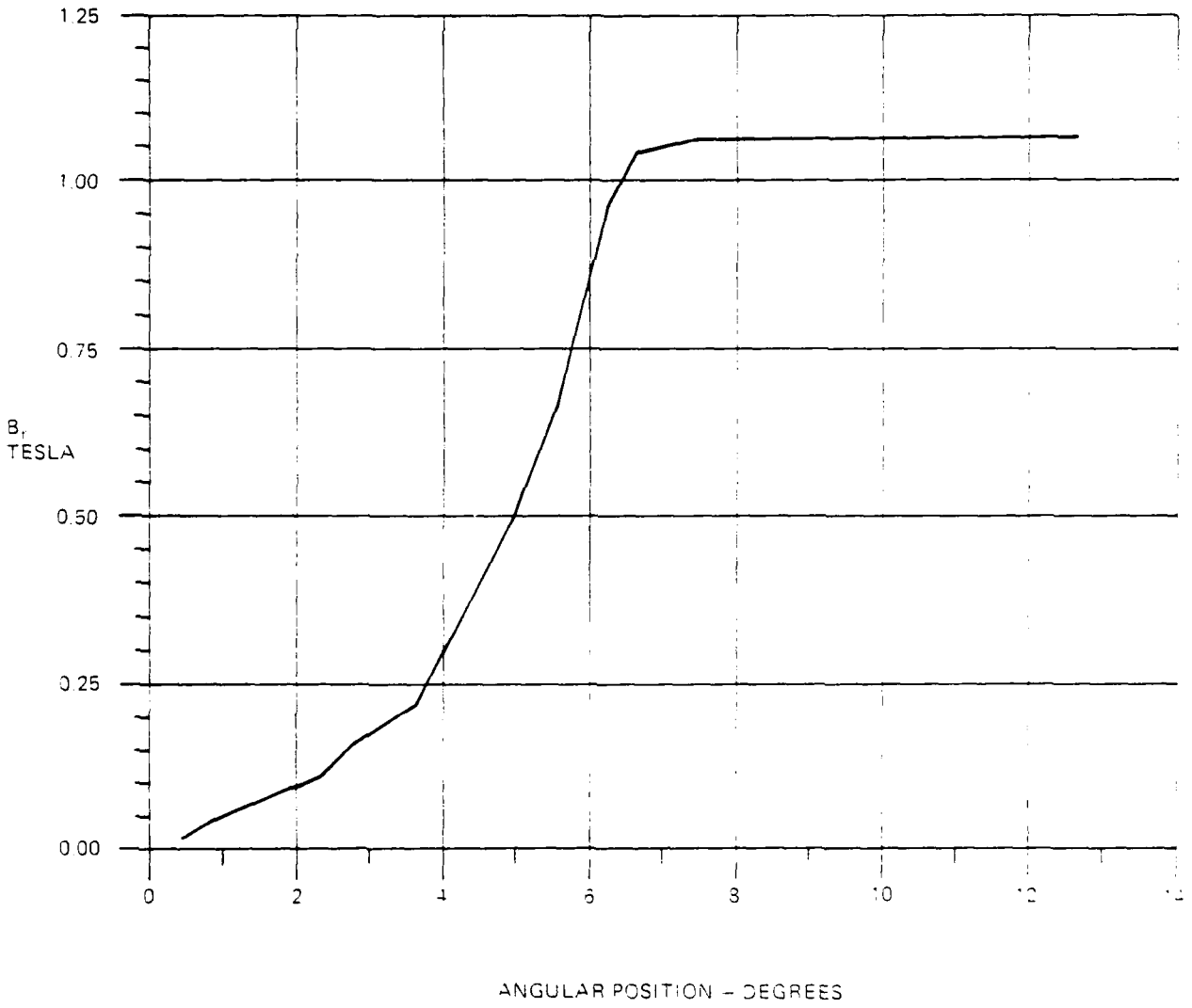

Figure 11. B_r at Stator Inner Radius for Uniformly Magnetized Magnet

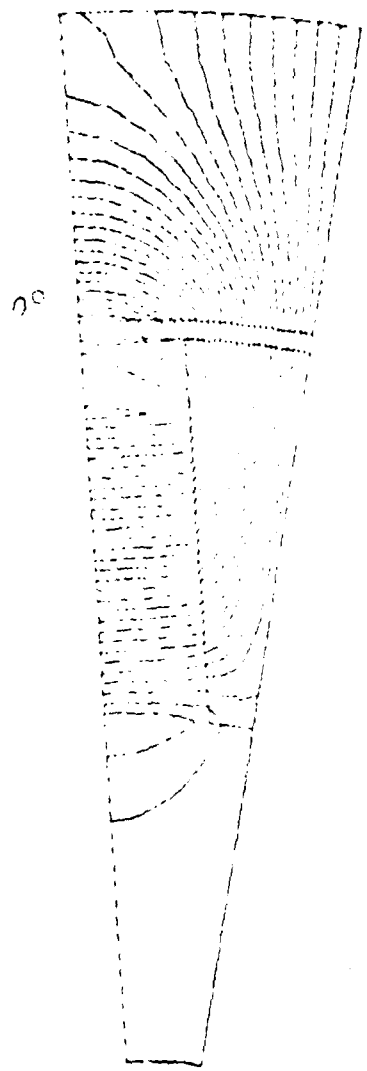

Figure 42. Flux Line Plot for Magnet with Magnetization Assigned from Defined Function

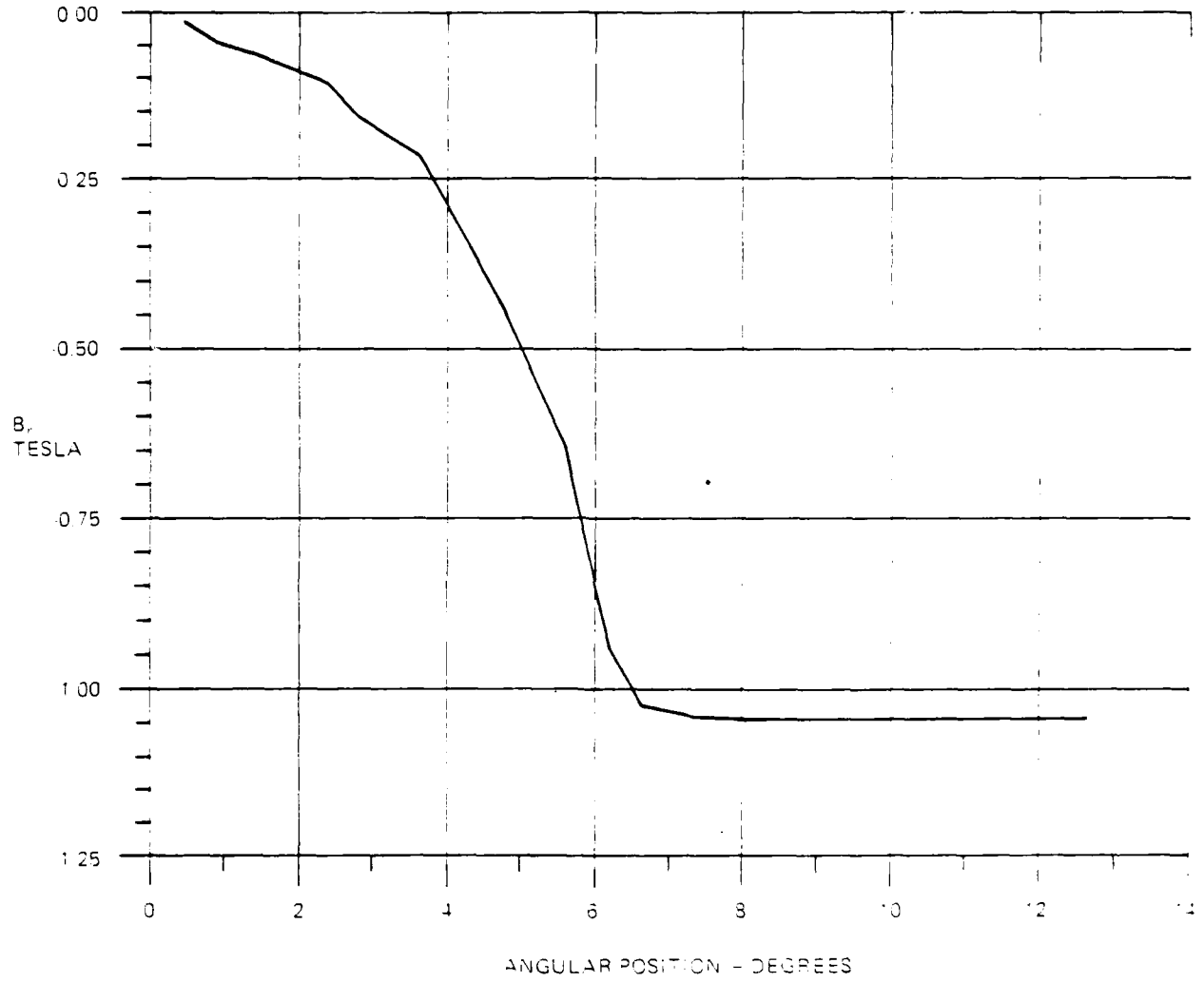

Figure 13. B_r at Stator Inner Radius for Magnet Magnetized in Complex Rotor Structure

(4) FEA Conclusion

It appeared from these numerical investigations that magnetization of complex rotor structures are feasible. The non-uniform magnetization does not appear to affect the resulting magnet performance with regard to flux density in the air gap. A note of caution should be mentioned here, for it is unclear what the effect of partial magnetization is on the temperature stability of the magnet. There does not appear to be much data in this area, and testing of the magnetized rotor structure over the specified temperature range is necessary to evaluate this effect.

The major question is whether the magnetizer power supply can deliver the necessary current to the magnetizer coils. This should be the focus of any further investigations.

e. Magnetization Fixture - Redesign

Based on the finite element analysis discussed in paragraph d., the magnetization fixture was redesigned. The redesigned fixture is shown in Figures 44 and 45.

f. Magnetization Power Supply

While the finite element analysis and fixture design was in process, a search was made of industry to locate a power supply in existence with the following requirements:

> 2000 volts
< 37,000 amps for 8-msecond duration.

Various power supplies were located with a higher voltage capability to satisfy the current needs. Due to the confined space available for the magnetization fixture winding, a thin film polyimide insulation system was selected. Thus the voltage criteria was selected at 2000 volts peak which was considered feasible for the short time

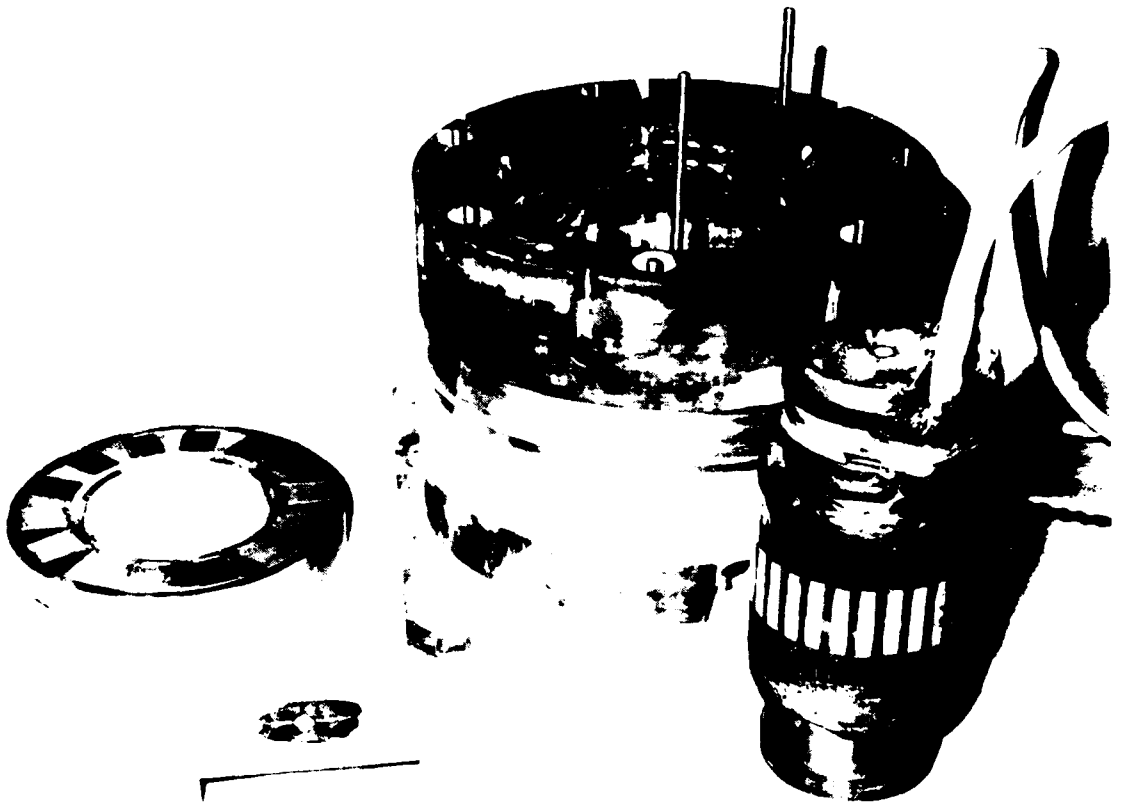

Figure 44. Magnetization Fixture - Redesign

Figure 45. Magnetization Fixture - Redesign with Rotor Disc Installed

exposure and life to complete this feasibility demonstration. Also the available winding space needed to minimize the inductance of the magnetization fixture required a small conductor run at a very high current density. Again this was thought to be feasible due to the short duration and short life of this technology demonstration.

Many power supplies were found with the voltage capability but due to fixture resistance and inductance these power supplies were determined not to have both the current and voltage capability simultaneously.

The power supply selected as being the one capable of meeting the above criteria was a corona test setup located at the Wilfred E. Skeets High Power Laboratory of the General Electric Company located at Philadelphia, Pennsylvania.

The selected power supply consisted of six banks of electrolytic capacitors composed of eight trays per bank with 48 capacitors per tray. Each bank was rated at 29,400 uf with 2000 volts charge capacity. Each tray had 12 taps to vary the inductance from 183 uh to 1770 uh. This inductance allowed the current to be limited and shaped. Each bank had the capability of being connected in series or parallel to vary voltage or capacitance value for the setup. Each bank had blocking diodes and an ignitron to discharge the capacitors as shown below.

g. Final Magnetization and Test - Final

The magnetization fixture, shown in Figure 44, was connected to the power supply described in paragraph f. During the preliminary check out pulses, to optimize the capacitor bank connections for current and waveshape, the magnetization fixture inner winding failed. Shown in Figure 46 is the current and voltage waveshape applied to the magnetization fixture prior to the failure. Figure 47 shows the current and voltage waveshape when the magnetization fixture experienced the failure.

The fixture was inspected and the inner winding end turns which had been tied and wrapped and then encapsulated with an epoxy compound were found to have become dislodged. Half of the inside magnetization fixture end turn winding were bent upwards at 90^{o}, see Figure 48, while the remaining end turns had become disjointed. See Figure 49. Some bulging was detected in the outer winding end turn area and the air gap areas showed signs of failure in the slot area. The rotor disc was found not to be damaged.

The rotor disc was tested after this failure. See Tables 14 and 15 for results. The approximate remagnetization level was 25%. Figures 50 and 51 show the voltage waveshape from the final magnetization.

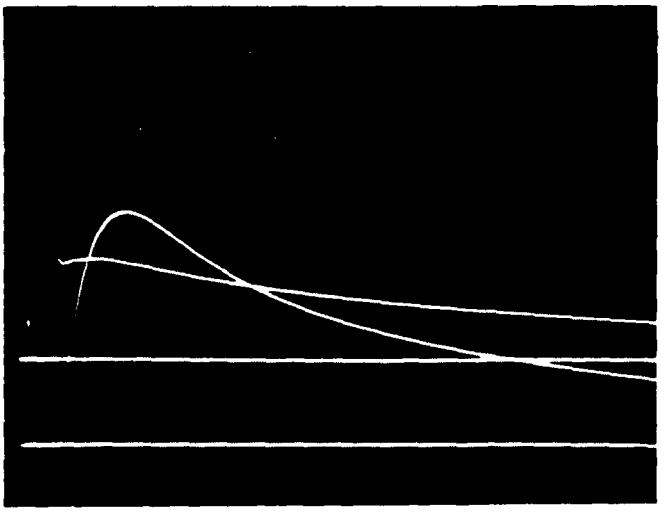

2ms/cm
500V/cm
4K Amps/cm
I_{peak} = 14K Amps
V_{peak} = 1K Volt

Figure 46. Magnetization Current and Voltage Waveshape

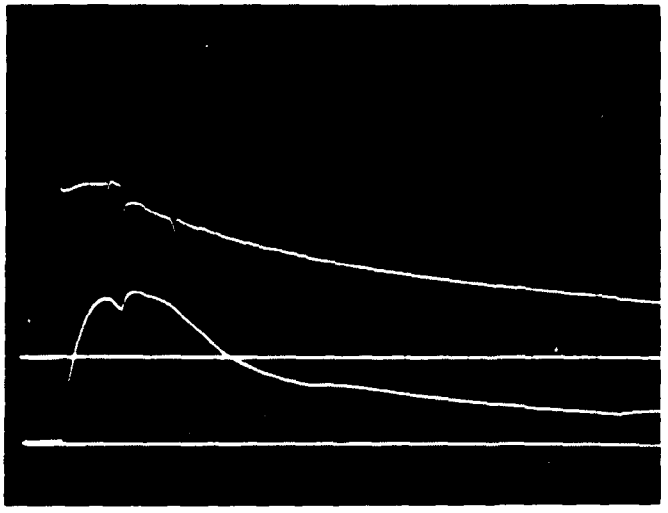

2ms/cm
500V/cm
10K Amps/cm
I_{peak} = 23K Amps
V_{peak} = 1.2K Volts

Figure 47. Magnetization Current and Voltage Waveshape During Failure

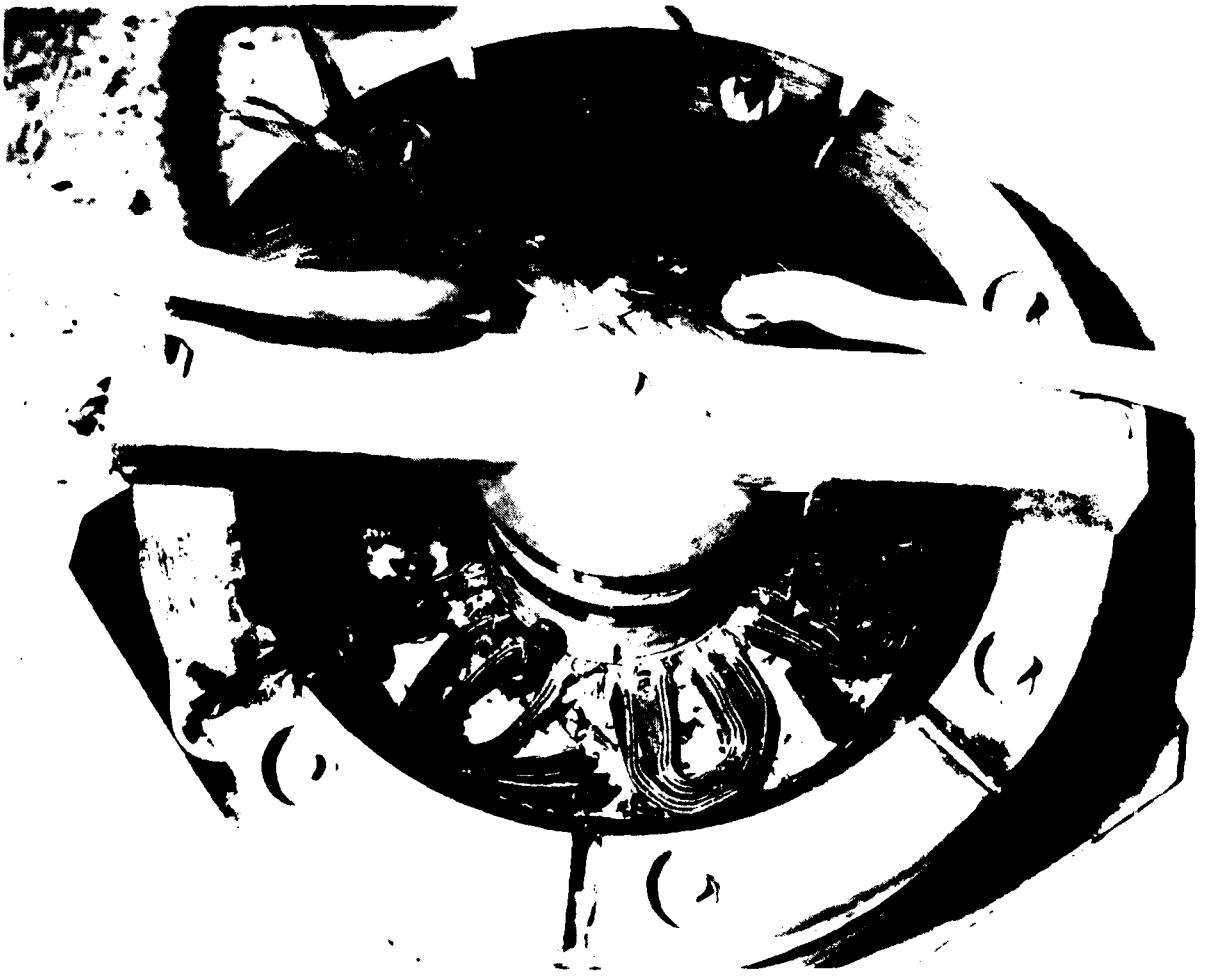

Figure 48. Failed Magnetization Fixture Inner Windings Dislocated 90°

Figure 19. Failed [illegible] Fixture Inner Winding [illegible]

TABLE 14

FLUX MEASUREMENT OF THE ROTOR DISC ASSEMBLED DEMAGNETIZED - FINAL MAGNETIZATION

POLE NO.	FLUX METER READING IN VOLTS	FLUX PER POLE (FLUX METER CONSTANT 1V = 100K LINES)
1	0.470V	47,000 lines
2	0.355V	35,500 lines
3	0.450V	45,000 lines
4	0.230V	23,000 lines
5	0.390V	39,000 lines
6	0.151V	15,100 lines
7	0.370V	37,000 lines
8	0.235V	23,500 lines
9	0.468V	46,800 lines
10	0.192V	19,200 lines
11	0.460V	46,000 lines
12	0.170V	17,000 lines
13	0.427V	42,700 lines
14	0.140V	14,000 lines

TABLE 15

GENERATED L-N VOLTAGE OF ROTOR DISC ASSEMBLED DEMAGNETIZED MAGNETS - FINAL MAGNETIZATION

SHAFT SPEED	GENERATED VOLTAGE	GENERATED VOLTAGE FREQUENCY
1000 RPM	0.586 Volts	117 HZ

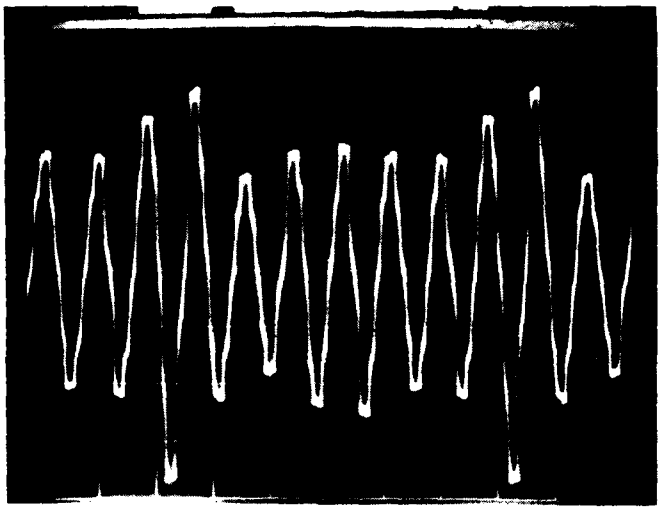

Figure 50. Generated Voltage Waveshape - Pull Coil Final Magnetization

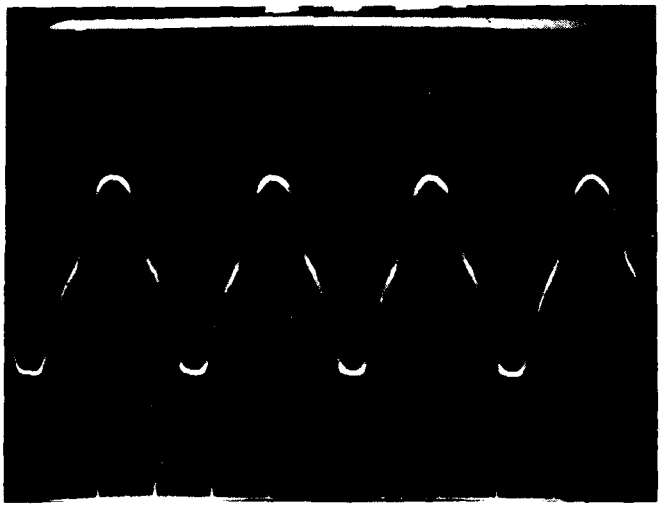

Figure 51. Generated Voltage Waveshape - Stator Winging Final Magnetization

SECTION IV

DISCUSSION

1. MAGNET DEMAGNETIZATION SELECTION AND EVALUATION OF MAGNETS

The specifications for the magnets used in this study were as follows: B_r>9200 gauss, H_c>8500 Oersteds, and $(BH)_{max}$>20 MGOe. The as-received magnets were from a batch that supposedly met the specifications; however, based on measurements accomplished, six of the magnets failed on the basis of B_r and two of the six magnets failed due to low energy product $(BH)_{max}$. This is not to imply that the vendor shipped magnets that did not meet the specification. Rather, it is more likely that variability in magnetic measurements accounts for the difference. It is unlikely that two measurement systems will agree closer than $\pm 1\%$ on B_r or H_c and $\pm 2\%$ on $(BH)_{max}$, so it should not be surprising that some magnets accepted by one measurement group will be rejected by another.

The question is how to minimize disagreements? In this study the open-circuit magnetization, $4\pi J_o$, was used as-measured with a Helmholtz detection system, to obtain information on the effect of temperature, and thermal demagnetization treatments. This was found to be a sensitive, reproducible method that takes only a few seconds for making the actual measurement. Another method used in this study was the extraction of the magnet from a close-fitting coil to provide data for calculating the open-circuit induction, B_o. In this method it is important to have a close-fitting coil. It was found that because of the small variability in the dimensions of the sample magnets, it was necessary to build the coil for the largest specimen. As a result, the coil was loose for the smallest magnets.

The design engineer starts with the B:H curve; however, in the final evaluation of the magnet quality, it is not necessary to measure the fixture B:H curve. A single measurement may be sufficient. If it is

assumed (in the present study) that the most important magnetic specification is the $(B:H)_{max}$ value, then either the $4\pi J_o$ or B_o value is sufficient to evaluate the magnetic quality for acceptance or rejection.

In Figures 19 and 52 the relation between $4\pi J_o$ and $(BH)_{max}$, and B_o and $(BH)_{max}$ is given. Thus it would be possible to use either B_o or $4\pi J_o$ measurements as a basis for accepting or rejecting a magnet instead of measuring the B:H curve in order to obtain the $(B:H)_{max}$ value. For example, in Figures 19 and 52, a B_o value greater than 5950 gauss and a $4\pi J_o$ greater than 9100 gauss would be equivalent to a $(B:H)_{max}$ value greater than 20 MGOe. Furthermore, it seems advisable to specify that the peak magnetizing field for the acceptance test be identical to that to be used in the in-place magnetization fixture.

2. REMAGNETIZATION FIXTURE

The extremely high magnetization ampere-turns necessary to expose the magnets of the rotor disc to a sufficient magnetization level requires the fixture to be capable of withstanding very high forces. These forces are particularly high in the magnetizing conductor in the end-turn area. This task is made doubly difficult since metallic support susceptible to eddy current induction during magnetization, should not be used. Also the space, particularly for the winding inside the ro-rotor inside diameter, is severely restricted because of the rotor disc geometry.

The above difficulties coupled with the very high powered, high voltage magnetizer required for magnetization of this particular complex rotor structure is theoretically possible. The results of this study indicate that achieving remagnetization may be impossible from a practical sense.

SECTION V

RECOMMENDATION

1. DEMAGNETIZATION AND REMAGNETIZATION

The equipment used in this study for thermal demagnetization consisted of a furnace surrounded by two large magnetizing coils. In the design of a manufacturing facility for thermal demagnetization it is recommended that the demagnetizing solenoid, or system, be separate from the furnace. The important factor is that the specimen be hot (e.g. 450°C) when exposed to the ac or dc field.

Another option is to expose the magnet to a demagnetizing field greater than the nominal H_{ci} before heating the specimen to a temperature near 450°C rather than the reverse practice.

In the selection of magnets for a magnetization-in-place program, it is recommended that the peak magnetizing field be no higher than the expected field to be realized in the in-place magnetization fixture.

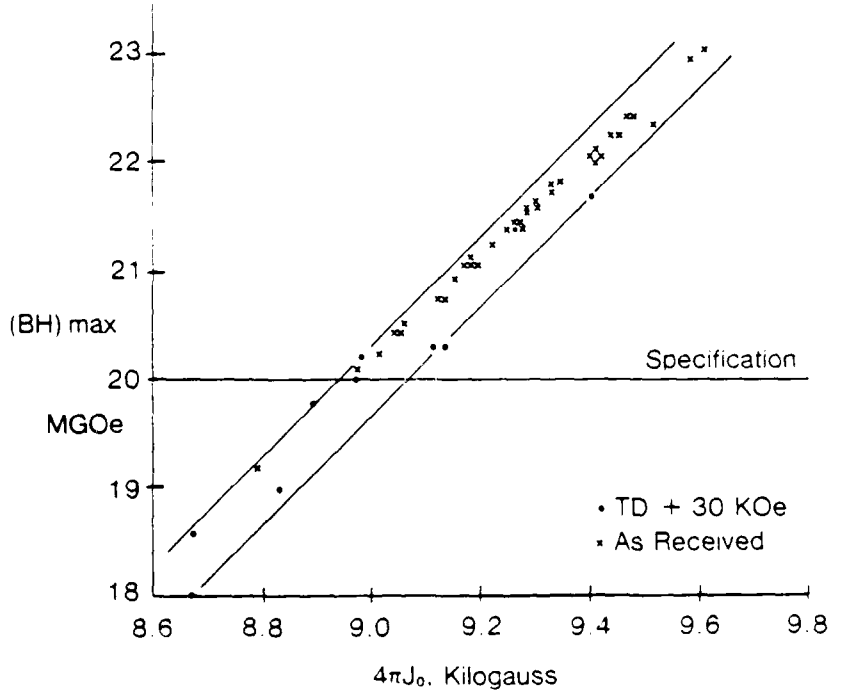

Figure 52. Data Showing Relationship Between B_o and BH_{max}

REFERENCES

1. M. G. Benz and D. L. Martin, "Measurement of Magnetic Properties of Cobalt-Rare Earth Permanent Magnet," IEEE Trans. on Magnetics, MAG-7, 285, 1971.

2. H. Zijlstra, Experimental Methods in Magnetism, Part 2, John Wiley & Sons, New York, pp. 79-84 and 102-108, 1967.

3. D. L. Martin and M. G. Benz, "Magnetization Changes for Cobalt-Rare Earth Permanent Magnet Alloy When Heated up to 650°C," IEEE Trans. on Magnetics, MAG-8, 35, 1971.

4. R. I. Joseph, "Ballistic Demagnetizing Factor in Uniformly Magnetized Cylinders," J. Appl Phys., 37, 4639, 1966.

5. D. L. Martin and M. G. Benz, "Temperature Dependence of Coercivity for Co-Sm Permanent Magnet Alloys," IEEE Trans. on Magnetics, MAG-8, 562, 1972.

6. D. L. Martin and R. J. Parker, "Demagnetization of Cobalt-Rare Earth Magnets," US Patent No. 3 802 935, April 9, 1974.

7. H. Mildrum and D. [illegible]en, Goldschmidt Informient, 4/75, No. 35, Page 54, 1975.


DAT
FILM